Plane-based Object Categorisation using Relational Learning: Implementation Details and Extension of Experiments

Reza Farid Claude Sammut

School of Computer Science and Engineering
University of New South Wales, Australia
{rezaf,claude}@cse.unsw.edu.au

Technical Report
UNSW-CSE-TR-201416
May 2014

THE UNIVERSITY OF
NEW SOUTH WALES

School of Computer Science and Engineering
The University of New South Wales
Sydney 2052, Australia

Abstract

Object detection, classification and manipulation are some of the capabilities required by autonomous robots. The main steps in object recognition and object classification are: segmentation, feature extraction, object representation and learning. To address the problem of learning object classification using multi-view range data, we use a relational approach. The first step is to decompose a scene into shape primitives such as planes. A set of higher-level, relational features is extracted from the segmented regions. Thus, features are presented in three different levels: single region features, pair-region relationships and features of all regions forming an object instance. The extracted features are represented as predicates in Horn clause logic. Positive and negative examples are produced for learning by the labelling and training facilities developed in this research. Inductive Logic Programming (ILP) is used to learn relational concepts from instances taken by a depth camera. As a result, a human-readable representation for each object class is created. The methods developed in this research have been evaluated in experiments on data captured from a real robot designed for urban search and rescue, as well as on standard data sets. The results show that ILP is successful in recognising objects encountered by a robot and are competitive with the other state-of-the-art methods.

In this report, we provide details of this plane-based object categorisation using relational learning, including the details of the developed segmentation method for producing high-quality planar segments used for learning object classes, implementation of features extraction, and specification needed for learning. We also perform some experiments to evaluate the new features and compare our method with a state-of-the-art non-relational object classifier.

1 Introduction

There are many applications that require machines with abilities close to those of human efficiency and consistency in understanding, interpreting and representing the world [1, 2]. Many industries, including agriculture, healthcare, medicine, mining, construction, virtual reality, entertainment, aviation and defence, make use of robots and artificial intelligence. The potential benefits of these technologies have a considerable impact on industry and the community by avoiding dangerous situations for humans by assigning parts of a task to a machine. Such a machine must be able to understand its environment and the semantics of complex objects, considering sub-parts and the functions of objects. The robot may be required to detect the existence of objects, recognise them and avoid or manipulate them.

The current research is motivated by urban search and rescue (USAR), where a team of robots is sent to a disaster site. These robots are expected to navigate the site autonomously and, using captured data, find significant features, recognise and classify objects like victims, floors, walls and furniture. The scene might include some data that do not belong to the object of interest (cluttering) or a part of an object surface might be absent due to occlusion [3]. The robots are designed to return a human readable, annotated map [4] showing their findings such as recognised objects [5, 6, 7, 8, 9], and especially, to locate victims and to report their condition [10].

The focus of our research is to use machine learning to build an object classifier for an autonomous robot in an urban search and rescue operation. Time of flight sensors, such as laser range finders, radar and sonar, are often used to obtain 3D data for mobile robotics applications, producing data in the form of a polygonal mesh and point cloud [11, 4, 12]. Therefore, 3D range images, or their corresponding point clouds, which represent a partial view of the environment, are assumed to be the primitive input.

3D depth cameras, such as the Microsoft Xbox Kinect, are now widely used because they provide both range and video images and their cost is much reduced compared with previous generations of similar cameras. In a range image, each pixel's value represents the distance of the sensor to the surface of an object in a scene from a specific viewpoint [13, 14]. This can be used to infer the shape of the object [15]. The Kinect, also incorporates a colour video camera but in this research, we only use the depth information for object recognition as colour calibration under different lighting conditions is problematic [1]. A range image can be transformed into a set of 3D coordinates for each pixel, producing a point cloud. Figure 1.1 shows a range image of a staircase with four steps, taken by a robot positioned in front of the staircase. In this grey scale image, the darker colour represents closer surfaces. For clarity, a colour-mapped version is also presented. The figure also includes front and top views for the same point cloud. The point cloud has been segmented into planes that are identified by unique colours. A range image only provides a partial view of a scene, since it is taken from one viewpoint. Constructing a complete 3D point cloud for an object requires multiple views.

In our early work [16, 17, 18], we extracted planes from the 3D point cloud based on a region growing plane segmentation algorithm [16] and used them as primitives for object categorisation. Planes are useful in built environments, including urban search and rescue

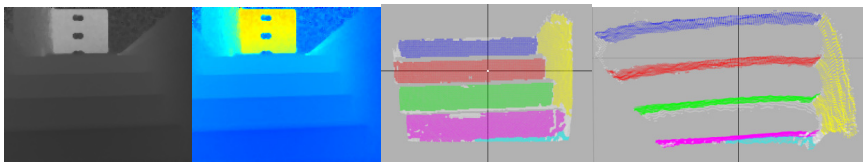

Figure 1.1: Range image and its correspondent point cloud (coloured) from front and top view

for identifying floors, walls, staircases, ramps and other terrain that the robot is likely to encounter. Modelling a scene from planar patches are used in computer vision, robotics and augmented reality [19]. For example, it has been used for scene understanding [20, 21], localisation [22] and 3D virtual reconstruction of the environment [23]. In this report, we provide details of implementation of the plane segmentation method, feature extraction and configuration for the ILP system used for the learning. Also, we add new features and perform new experiments to evaluate them. In the following sections, we describe the details of segmentation method, the features for extraction, the learning algorithm and the additional experimental results that demonstrate the utility of this approach. We also provide more detail of the system architecture and implementation.

2 The Overall Architecture

The overall system architecture can be decomposed into three general functions:

1. Data gathering: This covers different methods to obtain input images for the system.
2. Pre-processing, feature extraction and labelling: This is mostly performed by the GUI implemented for this research and the configuration files.
3. Learning and evaluation: This is performed outside of the GUI and is controlled by shell scripts that invoke external programs, including ALEPH [24].

Figure 2.1 illustrates the method. Note that there are some alternative labelling scenarios. In one case, the user can label the result of segmentation to form an object. In the second case, it is assumed that the input point cloud includes just one object and all segmented regions form the object. Therefore, automatic labelling is possible if the name of the object for a batch of data is provided. The output of labelling is a set of examples for each object class. For learning and evaluation, the examples are split into training and test sets by using 10-fold cross-validation in our experiments.

The Platform

All programs have been implemented on Ubuntu 12.04. For some experiments, we augment the software infrastructure developed by Team CASualty for controlling rescue robots. This has two main components: ‘robotserv’ runs on the robot, performing the time-critical tasks for control and perception. ‘robotgui’ runs on a base station, providing an operator interface and also performs compute-intensive tasks, such as simultaneous localisation and mapping.

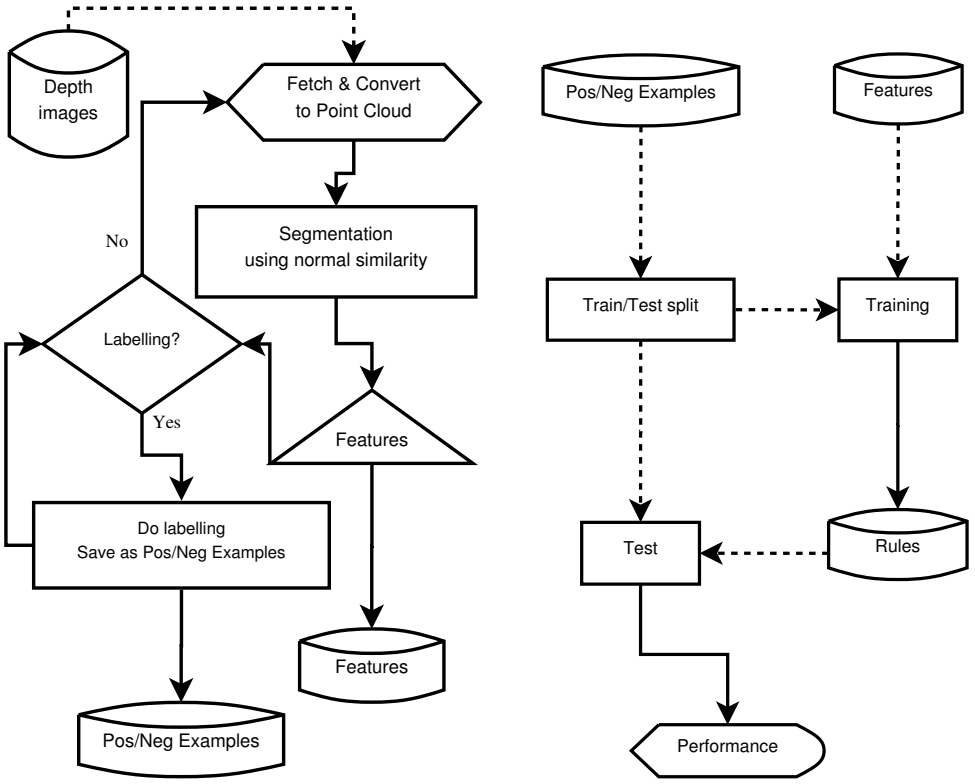

(a) Segmentation, Feature Extraction and Labelling

(b) Learning and Evaluation

Figure 2.1: Experimental setup in this research

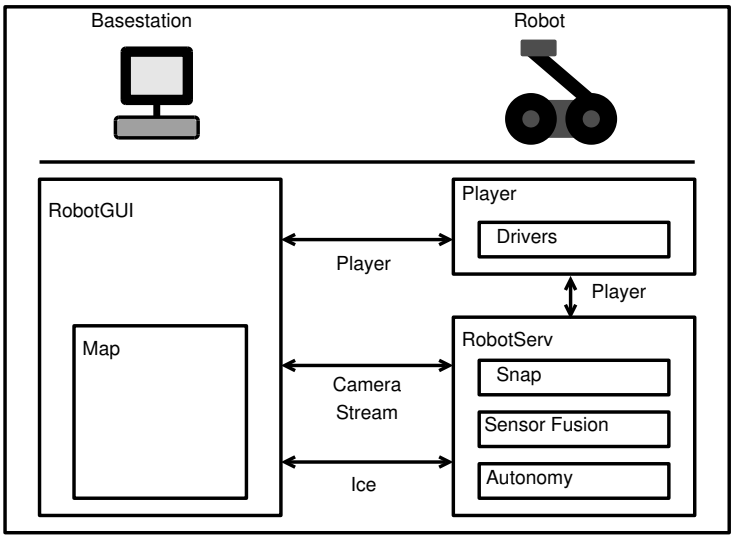

Figure 2.2: An overview of Team CASualty's platform and its communication channels

Both components are configured by an XML file, which specifies which sub-systems are to be used and their settings. Figure 2.2 shows an overview of this platform and its communication channels.

We will provide more related details later in Section 8. Next five sections focus on segmentation, feature extraction and representation, the language specification used for learning and new experiments for evaluation.

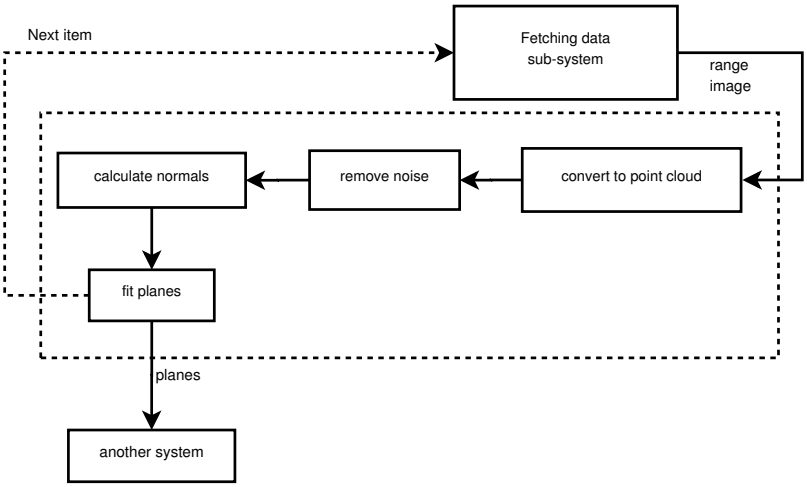

Figure 3.1: Illustration of plane segmentation steps and its communication with others

3 Segmentation

We use the plane as the primitive for describing objects, where an object is considered to be composed of a set of planes derived from a point cloud. To find these planes, each point's normal vector is calculated and used to segment the point cloud. That is, neighbouring points are clustered by the similarity of their normal vectors. A schematic view of the use of plane segmentation is shown as Figure 3.1. Figure 1.1 shows an example of planes found using this method.

3.1 Range Image to Point Cloud

A range image can be transformed into a set of points in 3D space, producing a 3D point cloud [25]. Figure 3.2 shows the corresponding point cloud for Figure 1.1. Because using just one view, such as the front view (Figure 3.2a) is ambiguous, the other views of the same point cloud are also shown. Some points in this point cloud are removed because they are far away, such as the points in the yellow region of the colour-mapped version in Figure 1.1.

After this conversion, an ordered (or structured) point cloud is available. Due to the 2D nature of the range image, the neighbourhood of each point in the ordered point cloud can be easily and quickly found. This fact has a great impact on the preprocessing speed. However, it should not be considered a limitation. Many algorithms create a neighbourhood structure when the point cloud is unordered. Therefore, the input is not be limited by range images. Any point cloud representing a partial view of an object can be used similarly.

A point cloud can be produced by converting a range image into a set of 3D points. Each pixel in a range image has a 2D coordinate (X,Y) and a depth value, d. The pixels must be projected onto a 3D (X, Y, Z) coordinate system in the robot's frame of reference. We use a routine provided by Team CASualty [26, 27, 28] in their CASrobot software libraries created for RoboCup Rescue. Lai et al. [29] also provide a MATLAB code[1] for the same purpose.

[1] http://www.cs.washington.edu/rgbd-dataset/software/depthToCloud.m

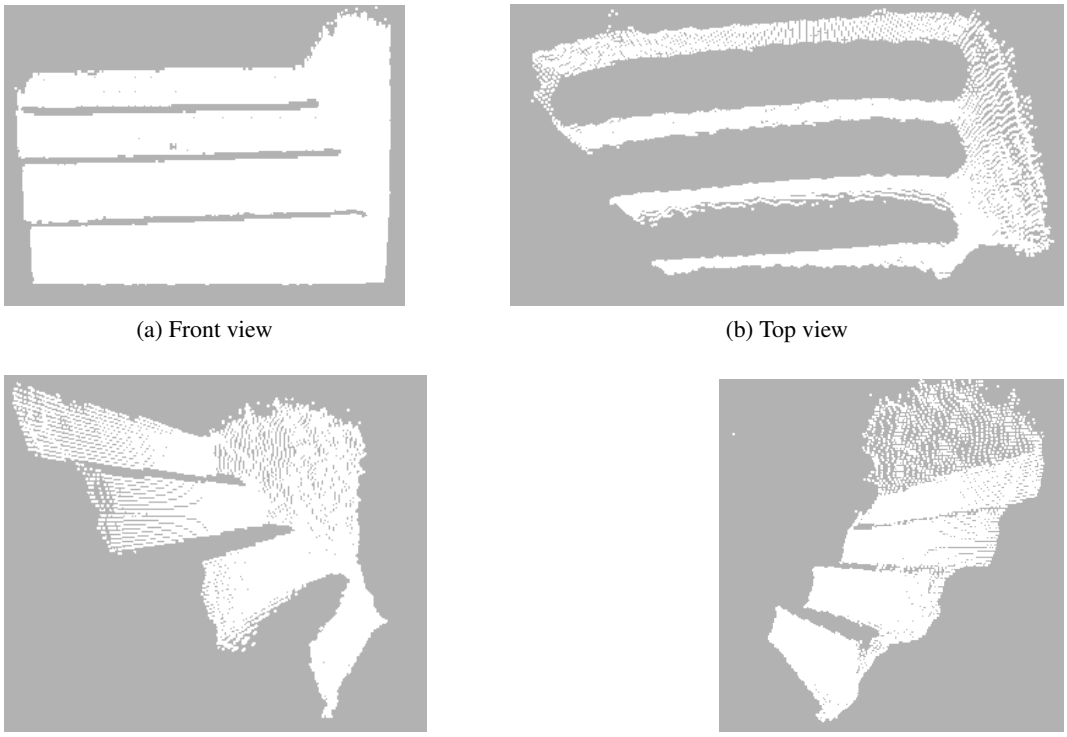

(a) Front view

(b) Top view

(c) Left view

(d) Right view

Figure 3.2: Corresponding point cloud for range image captured by SwissRanger SR3000 positioned in front of a staircase with four steps (Figure 1.1)

3.2 Plane Segmentation Algorithm

We developed a region growing plane segmentation algorithm in our early work [16] that did not include using a distance threshold. In this report, we update that algorithm and add the distance threshold criterion. The main idea of this region growing algorithm is that neighbouring points with similar normal vector values can form a region and will be represented as a plane. The method starts with a point and traverses the other points through the neighbourhood structure. To decide if the point can be added to the planar surface, it must satisfy the planar surface criteria, given below.

We have used the below values for input variables:

`min_neighbour_num = 4`

`base_update_step = 8`

`num_initial_points = 16`

$\theta = 15^\circ - 20^\circ$

The region growing criteria determine when to add a point to a region. Our algorithm is based on using neighbouring points to grow the region. This is where the distance threshold, δ, can be used to decide whether a point is too far away to be accepted as a neighbour for a point. If a point is not too far, it can be included in the *not visited neighbours* list, *candidates*, as shown in the algorithm.

Algorithm 1 Region growing plane segmentation algorithm using normal vectors

Input: $PointCloud$
Input: $min\_neighbour\_num > 0$
Input: $base\_update\_step > 0$
Input: $num\_initial\_points > 0$
Input: min_region_size // minimum region size
Input: θ // angle threshold
Input: δ // distance threshold
Input: $angle\_mf < 1$ // angle modifying factor
Input: $normal\ vector\ for\ all\ points\ in\ PointCloud$

$R \leftarrow \{\}$ // output: Regions
for all p in the PointCloud **do**
  if $p\ is\ visited \vee p\ is\ rejected$ **then**
    continue
  else if $number\_of\_usable\_neighbour(p) < min\_neighbour\_num$ **then**
    continue
  end if
  $C_R \leftarrow p$
  $Base\_normal \leftarrow get\_normal\_vector(p)$
  $candidates \leftarrow get\_not\_visited\_neighbours(p, \delta)$
  for all q in candidates **do**
    if $Size(C_R) < num\_initial\_points \vee mod(Size(C_R), base\_update\_step) = 0$ **then**
      $Base\_normal \leftarrow get\_average\_normal\_vectors(C_R)$
    end if
    $current\_angle \leftarrow get\_angle(Base\_normal, get\_normal\_vector(q))$
    $accepted \leftarrow$ **false**
    if $Size(C_R) < num\_initial\_points$ **then**
      if $current\_angle < \theta$ **then**
        $accepted \leftarrow$ **true**
      end if
    else if $current\_angle < \theta * angle\_mf$ **then**
      $accepted \leftarrow$ **true**
    end if
    if $accepted$ **then**
      $C_R \leftarrow C_R \cup q$
      $set\_visited(q)$
      $candidates \leftarrow candidates \cup get\_not\_visited\_neighbours(q, \delta)$
    end if
  end for
  if $Size(C_R) > min\_region\_size$ **then**
    $set\_final\_normal\_vector(C_R)$
    $R \leftarrow R \cup C_R$
  end if
end for
return R

(a) Colour version, the area having similar normals are highlighted

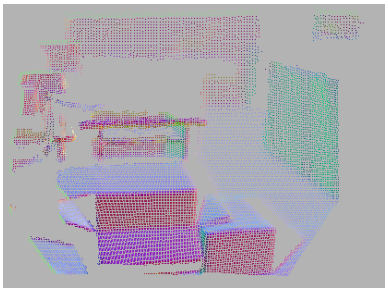

(b) Normals are represented by RGB colour

Figure 3.3: The top side of box and the ground have similar normal vectors

(a) Colour version; the area having similar normals are highlighted

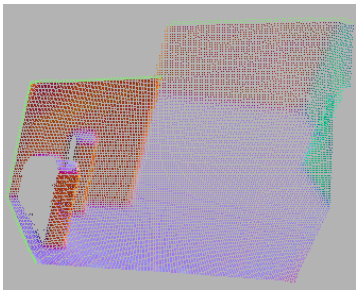

(b) Normals are represented by RGB colour

Figure 3.4: Another example when part of the two object surfaces have similar normal vectors

3.2.1 Calculating the Distance Threshold

In this section we explain how this threshold can be calculated. Since the segmentation algorithm uses a point's neighbours for growing the region, there is a chance that a neighbouring point might have a normal vector close to the current point, even though it belongs to another region. This may occur on edges because of the sensor's point of view as shown in Figures 3.3 and 3.4. For both figures, we have provided a colour version of the scene, highlighting the area which such issue has happened. Also a point cloud version of the scene is provided when the RGB colour of each point is formed by the normal vector of the point. Figure 3.3 shows such situation for a top surface of a box and the ground, while Figure 3.4 illustrates the same for two situations where a side of a box and the wall are having parallel normal vectors and also another wall has parallel normal vector with one side of a wooden stick. A distance threshold may avoid such points, having parallel normals, but are too distant, however, it is difficult to define *too far* or *too distant*.

Turk and Levoy [30] suggest a method for building a triangular mesh from a range image using a distance threshold. If a point is too far from another point, no edge connects them in the mesh. Range points are flattened by not including depth information, which is using X,Y values and ignoring Z values. Next, the maximum distance between adjacent range points, s, is determined. Finally, the distance threshold, $4s$, is defined. The idea is shown in Figure 3.5.

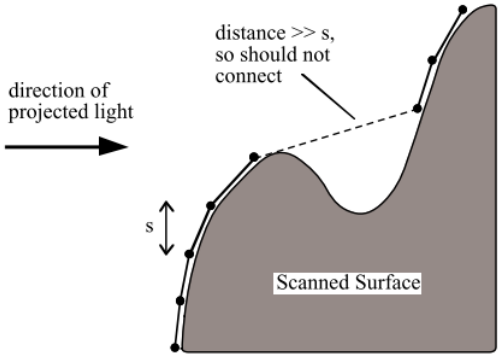

Figure 3.5: Illustration of the idea for setting distance threshold to build a mesh from range points

[30]

Although this thresholding mechanism does not work on our data, the same idea can be applied to another statistical component. We do not flatten the range data, instead, the minimum distance between each point and its adjacent neighbours is calculated. Next, the average of these minimum values, *s*, is found. Similar to the above method, *4*s is used as the distance threshold.

Figures 3.6 and 3.7 show some instances of segmentation with and without using distance thresholds. The front view of segmentation with bounding convex hulls and oriented bounding boxes is shown in the first figure. The top surface of one of the boxes is merged with the ground as one planar surface when the distance criterion is not used. Incorporating the distance criterion avoids this problem and better bounding for the related regions can be achieved. A similar situation occurs in Figure 3.7. Here, the front and top views are shown for the convex hull for regions and the oriented bounding boxes from the front view. We compared segmentation, with and without the distance threshold, for **105** images containing *stairs*. The segmentation of **69** images are improved and become closer to human manual segmentation when employing the distance threshold.

3.2.2 Setting Minimum Region Size

Another parameter is used in this algorithm, that is the minimum region size. If the size of a region, which is the number of points belonging to that region, is less than a threshold, the region is rejected. It is important to set this threshold based on the range camera used for capturing data. For this purpose, a comparable parameter such as *camera density* is determined, which represents the relative number of pixels due to the camera's field of view. We defined the camera density for SwissRanger SR3000 as 3.5, while it is 10.0 for Kinect and ASUS Xtion. Using this value, one minimum region size set for the SwissRanger SR3000 can be set for another camera such as the Kinect by using the ratio of their camera densities. Since the fields of view of the available cameras are given to the system, all modules can set these parameters simply by specifying the camera that was used to capture the image. Another factor to be considered is the sampling rate used to reduce the number of points in the point cloud for faster processing.

(a) Colour version of the scene

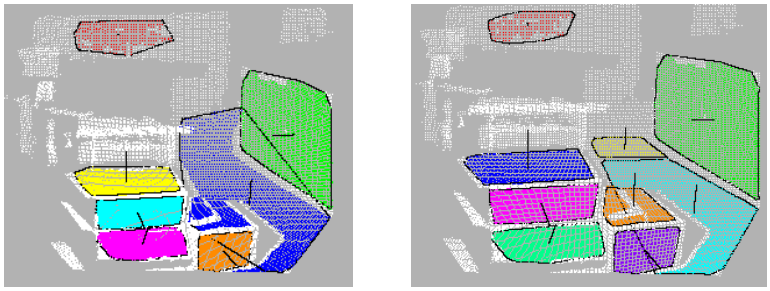

(b) Front view, bounding convex hull, without and with using distance threshold

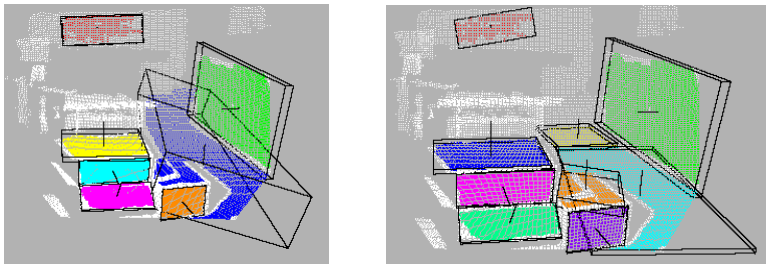

(c) Front view, oriented bounding box, without and with using distance threshold

Figure 3.6: Boxes in a scene, the effect of using distance threshold

To calculate an appropriate minimum region size, we use *min_region_size_base* as the base number of points for a range image taken by SwissRanger SR3000. This number is scaled down in respect to the sub-sampling rate used. This threshold is also scaled by the corresponding camera density. For example, we used 175 as the base value for planar objects in various experiments.

4 Feature Extraction

We have used the *plane* as the primitives for describing objects, where an object is considered to be composed of a set of these primitives derived from a point cloud. The point cloud is represented by a set of features extracted from these regions and by relationships between regions. These features and relations include: the attributes of each individual region, the relationships between every pair of regions, and features based on an aggregation of the regions. After extracting these features, sets of regions are labelled according to the class to which they belong. The ALEPH ILP system [24] is used to build a classifier for each class, where objects belonging to that class are considered positive examples and all other objects are treated as negative examples.

(a) Colour version of the scene

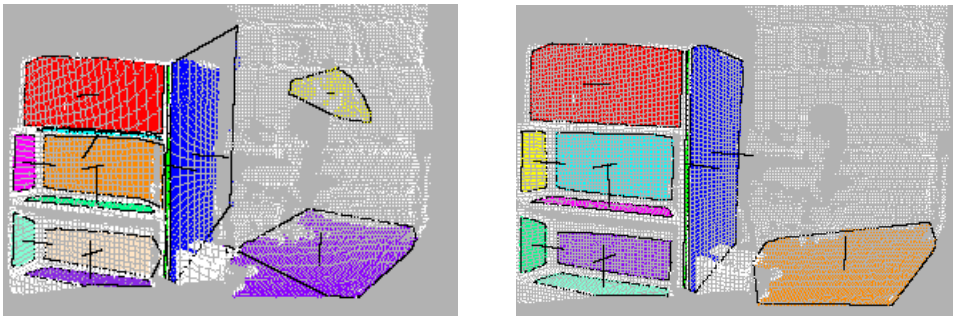

(b) Front view, bounding convex hull, without and with using distance threshold

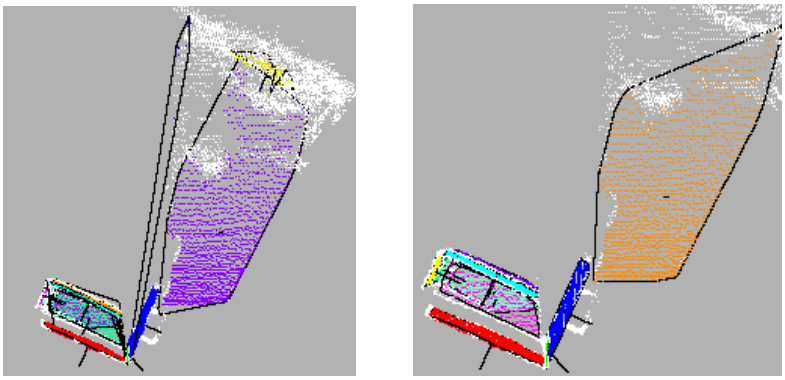

(c) Top view, bounding convex hull, without and with using distance threshold

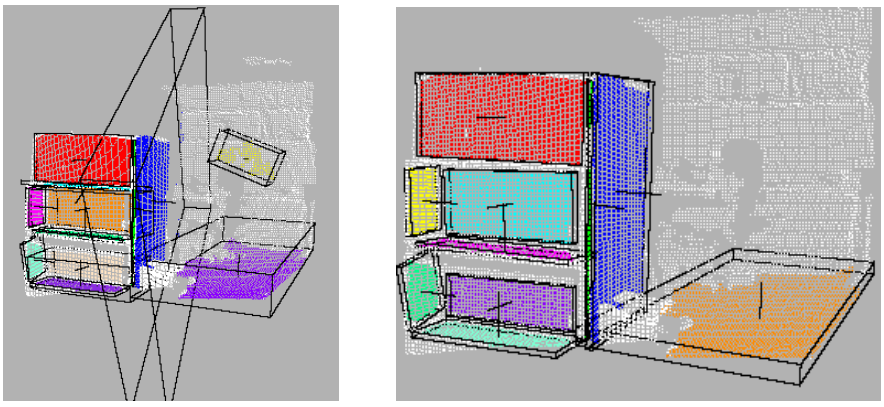

(d) Front view, oriented bounding box, without and with using distance threshold

Figure 3.7: Bookcase in a scene, the effect of using distance threshold

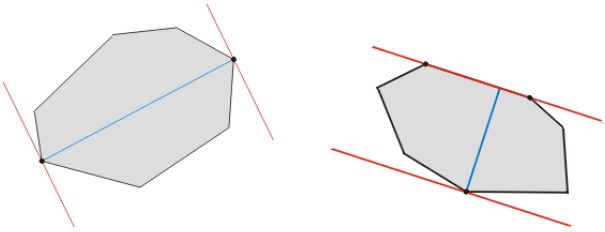

(a) Diameter (b) Width

Figure 4.1: Features of a convex hull

4.1 Single Region Features

4.1.1 Normal Vector:

The mass and normal vector of a planar region are the average of the points belonging to the plane and the average of their normal vectors, respectively. The normal vector is represented by its spherical coordinates (θ and ϕ) [31], where θ is defined as zero when x=y=0. The normal vector is normalised, so $\rho = 1$ for all cases.

4.1.2 Region Boundary

The boundary of a planar region can be represented by a convex hull [32]. For example, Tsai et al. [33] used convex hulls to form boundaries of planes. There are many convex hull algorithms [34, 35, 36, 37]. The method employed in this research is a modification of the Andrew's algorithm [38]. From the convex hull, two more features can be extracted: the diameter of the convex hull and the width of the convex hull. The former is the distance between two points on the convex hull that are furthest away [39]. The latter can be defined as the distance between two parallel lines containing the convex hull [40]. The width and diameter for a convex hull are illustrated in Figure 4.1. Calculating the ratio between these two features, another scale-invariant feature, ***convex_ratio***, can be created. Some algorithms [40, 41, 39] are described for finding the diameter and width of a convex hull. We use the source code[2] provided by Schneider and Eberly [42] that implements rotating calipers [41].

Since we are using range data and the point cloud does not show the whole 3D object shape, it is sufficient to find a 2D convex hull. The 2D convex hull algorithm introduced by Andrew [38] serves as a starting point. To fit a convex hull around a region, its points must be projected onto a 2D space. This is performed by projecting the region onto the smallest dimension of its oriented bounding box. After fitting the convex hull, it is projected back to 3D coordinates.

4.1.3 Bounding Box and Region Distribution

An additional feature is how a region is distributed. One way to calculate this is by using the bounding box and calculating the length of its three axes. By determining the difference between the maximum and minimum values of a region's point coordinates ($\triangle x$, $\triangle y$ and $\triangle z$) and comparing them, we decide along which axis the plane is distributed the most.

[2] http://www.geometrictools.com/LibMathematics/Containment/Wm5ContMinBox2.cpp

Another feature set consists of the ratios between each pair of the above values ($\frac{\triangle x}{\triangle y}$, $\frac{\triangle y}{\triangle z}$ and $\frac{\triangle x}{\triangle z}$), which is robust to scaling. These attributes are in the sensor's frame of reference and since they are not object-centred, rotating the object might affect them.

4.1.4 Oriented Bounding Box

Since region distribution does not consider orientation, it is useful to create an oriented bounding box for each region and to use its properties in the object description. To fit an oriented bounding box to each region, we use the method presented by Gottschalk [43] and implemented by Gregson [44].

Similar to $\triangle x$, $\triangle y$ and $\triangle z$, three values $\triangle d_i$ can be determined, which show how the region is distributed along the oriented bounding box axes (where $\triangle d_1 \geq \triangle d_2 \geq \triangle d_3$). However, of interest are the ratios $\frac{\triangle d_1}{\triangle d_2}$, $\frac{\triangle d_2}{\triangle d_3}$ and $\frac{\triangle d_1}{\triangle d_3}$. Since the oriented bounding box is robust to rotation, these ratios benefit from this robustness in addition to their scale-invariance.

Figure 4.2 shows the RGB-colour version of the scene, bounding boxes and oriented bounding boxes after the planar segmentation. Each region is represented by a different colour using the provided colour legend. In contrast to bounding boxes that are not object centred, oriented bounding boxes are object centred and can provide features that are invariant to transformation such as rotation. Since oriented bounding boxes were a later addition to our research, both feature sets are used separately in various experiments. Thus, bounding box features are introduced first, and are later replaced by oriented bounding boxes.

4.2 Region Relationships

The relationships between shape primitives describe the structure of an object and can be used to find similarities between instances of object classes. Thus, after finding segments and calculating their individual properties, relationships are constructed between each pair of primitives. These are in the form of how the regions are located with respect to each other and how their individual features can be compared.

4.2.1 Angle Between Two Regions

The angle between two regions is the angle between their normal vectors.

4.2.2 3D Spatial Relationship

Another relationship is based on binary topological [45] and spatial [46, 47] relationships such as the directional relationship [48, 49] that describes how two planes are located with respect to each other. For example, as shown in Figure 4.3, rectangle *b* is located on the *east* side of rectangle a, from the perspective of one 2D view. To find this direction between two rectangles, the line that connects both centres is used. The line that connects the centres of *a* and *b* is closer to the *east* axis defined on the centre of rectangle *a*. Thus, we say that *b* is east of *a*. This definition can be easily extended to other directions, *north-east*, *north-west*, *south-west* and *south-east*. Note that this relation is view dependent.

(a) Colour legend

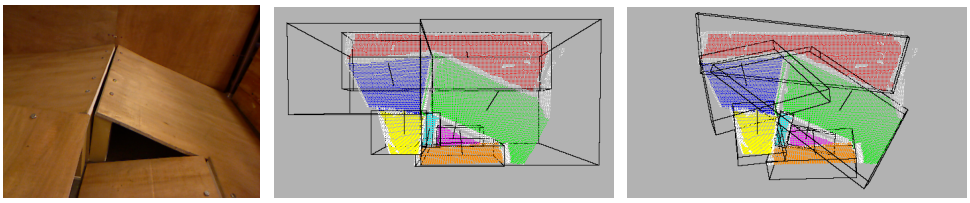

(b) Pitch/roll ramp

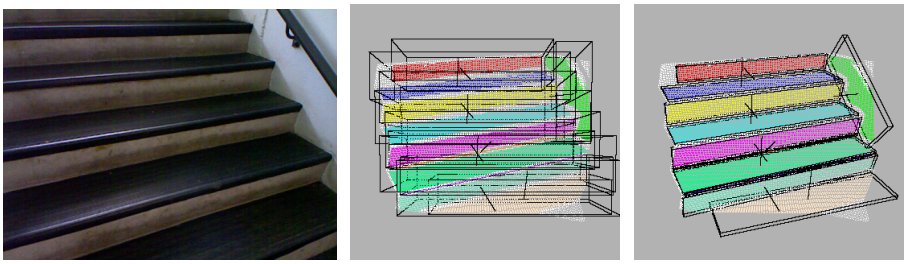

(c) Stairs

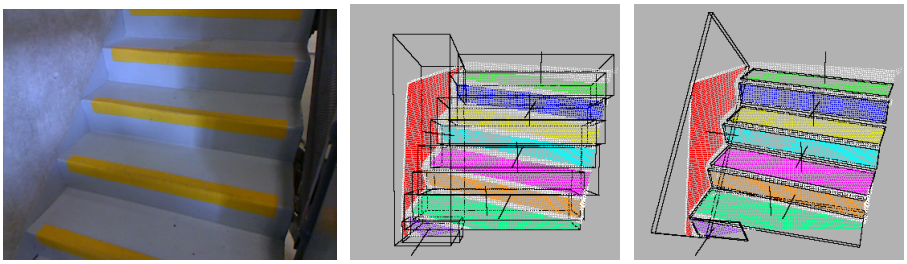

(d) Stairs

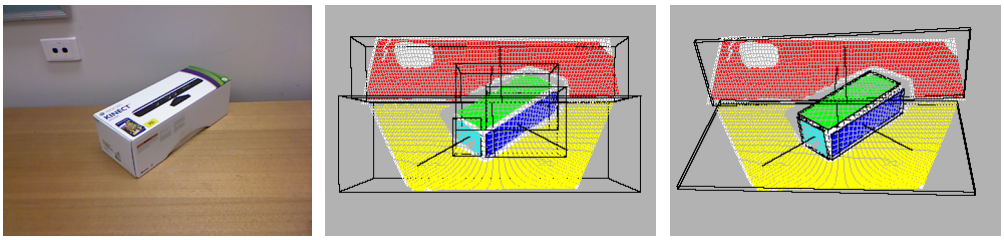

(e) Kinect box on the table

Figure 4.2: RGB-colour image (left), bounding boxes (middle) and oriented bounding boxes (right) for some selected objects. Each region is represented by a different colour using the provided colour legend.

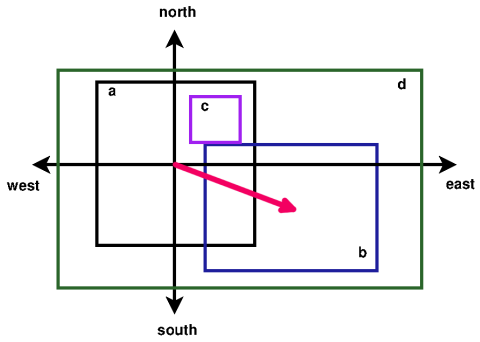

Figure 4.3: Example of spatial arrangement for four rectangles **a**, **b**, **c** and **d**

A further relationship is when two rectangles share partial edges or one rectangle covers the other. In this figure, rectangle a covers *c*, while rectangles *b* and c are connected. Also rectangle *d* covers all rectangles *a*, *b* and *c*.

This concept is defined for 2D space and requires some modification to be used for 3D space. Several researches have studied this kind of relationship. Borrmann et al. [50] define 3D spatial data types and their operators and devise a spatial query language. Berretti and Del Bimbo [51] propose a modelling technique for 3D spatial relationship, while Zlatanova et al. [52] give an overview of models for 3D topology. Ellul and Haklay [53] identify the requirements for 3D spatial relationships and Chen and Schneider [54] discuss this 2D to 3D generalisation and propose a neighbourhood configuration model to encode the topological relationship. We chose to test a simpler approach in this research. In Figure 1.1, two views of the same segmented 3D point cloud are shown: front view and top view. Both views are shown as 2D images. Regions that might not look parallel to each other from one view, are clearly parallel from another. The 3D view can be projected onto two 2D views to find the spatial-directional relationships in each 2D view. For this purpose, a bounding cube, with respect to the sensor's coordinate frame, is generated for each set of points assigned to a region. Two projections of this cube are then used to represent the minimum bounding rectangles for the region from each of the two views. The projections are on the XY plane (front view) and the ZX plane (top view). Referring to Figure 4.3, the X-axis represents the West to East and the Y-axis shows the South to North direction in the front view. For the top view, the X-axis is in the South to North direction while the Z-axis represents the West to East direction

It is possible that redundant relations will be generated for an object description. However, there are mechanisms for eliminating redundancies. For example, if the bounding rectangle of region X from a particular view is covered by the bounding rectangle of region Y, and region Z has another relationship with region Y, the relationship between region Z and X in that view is eliminated. This can be seen in the front view of Regions 1, 4 and 5 in Figure 4.2e. Region 5 is covered by Region 4, while there is another relationship between Regions 1 and 4. As a result, since the coverage relationship between Regions 4 and 5 dominates any possible relationship between Regions 1 and 5, the relationship between Region 1 and Region 5 is eliminated.

$$u = n_s \quad v = u \times \frac{(p_t - p_s)}{\|p_t - p_s\|_2} \quad w = u \times v$$

$$\alpha = v.n_t \quad \phi = u.\frac{(p_t - p_s)}{d}$$

$$\theta = arctan(w.n_t, u.n_t)$$

$$d = \| p_t - p_s \|_2$$

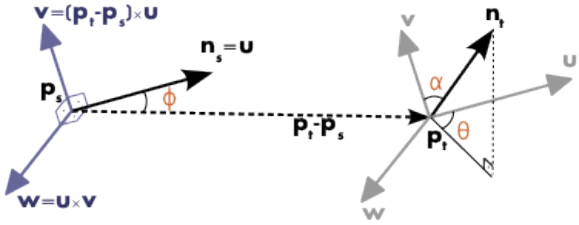

Figure 4.4: Relative difference between two masses and their associated normals [57]

4.2.3 Relative Difference Between Normal Vectors

Another region relationship is calculated from the difference between two centres of mass (p_s and p_t) that belong to two regions, using their associated normal vectors (n_s and n_t). This feature is used in the PCL [55] for creating Point Feature Histograms (PFH) [56]. The relationship is defined by a 4-tuple $< \alpha, \phi, \theta, d >$ and a coordinate frame at p_s as shown in Figure 4.4, where d is the Euclidean distance between two points.

4.3 Region-Set Features

Another category of features considers all regions that together form an object. For example, the *pitch/roll ramp* is formed by Regions 2 and 3 in Figure 4.2b, while Regions 2, 3 and 5 in Figure 4.2e form the *box*. In the case of the *stairs* in Figures 4.2c and 4.2d, the number of regions that make up the object class is not fixed as *stairs* may have a different number of steps. For example, region-sets (1,3,4,5,6) and (1,3,4,5) in Figure 4.2c form *stairs*. This can be handled by a recursive class description.

4.3.1 Number of Regions Forming an Object

Following the previous point, many objects will have a fixed number of regions visible in a particular view, therefore, the number of visible regions may be used as a feature. However, as noted above, in some cases that number is not always useful.

4.3.2 Oriented Bounding Box and Corresponding Ratios

Another feature can be calculated by making an oriented bounding box for the whole object. Similar to the single region feature, three ratios for each box are extracted.The third category of features is based on considering all regions that form an object.

Binning for Angle and Ratio values

We have used a binning system instead of using the exact value for angles and ratios. An angle will be represented by one of the following bins as 0±15, 45±15, 90±15, 135±15, 180±15, 22.5±15, 67.5±15, 112.5±15 and 157.5±15 or their negative corresponding.

Similar to binning used for angle values, ratios are **binned** in intervals defined around fixed values 1, 1.5, 2, 2.5, ... with the interval length 0.5 (i.e. ± 0.25). That is, they can be represented as:

$\{i \pm 0.25; i = 1, 1.5, 2, 2.5, 3, ...\}$

This binning system works for ratios ≥ 1 such as OBB ratios $\frac{\triangle d_1}{\triangle d_2}$, $\frac{\triangle d_2}{\triangle d_3}$ and $\frac{\triangle d_1}{\triangle d_3}$ which are always ≥ 1. When the ratio $\lneq 1$, and to avoid having small ratios such as 0.005, the concept of inverted ratio values is defined here.

The inverted ratio can be explained by an example. If $a \lneq b$ then $\frac{a}{b} \lneq 1$, and therefore $\frac{b}{a} \geq 1$. Instead of using the ratio $\frac{a}{b} \lneq 1$, we use $\frac{b}{a} \geq 1$. To show that we have applied this inversion, we represent the inverted ratios by a negative sign. For example, when $\frac{a}{b} = 0.78$, its inverted ratio is $\frac{b}{a} = 1.28$. This value (1.28) must be represented as 1.5 ± 0.25, however since it is an inverted version, its corresponding ratio bin will be represented as -1.5$\pm$0.25.

5 Feature Representation

The directional relationships of rectangles shown in Figure 4.3, can be expressed easily as Prolog facts. For example, the Prolog facts for some of the directional relationships in Figure 4.3 are:

```
east(a,b).   /* (rectangle) a is on the east side of b. */
covers(a,c), not_covers(a,b).
/* a covers c and a does not cover b. */
connected(b,c).   /* b is connected to c. */
covers(d,X). /* d covers all rectangles. */
```

Here, the names of the *relations* are ***east***, ***covers***, ***not_covers*** and ***connected***. The last clause, is not a ground fact. It is a generalisation that contains the variable ***X***, and *subsumes* the three ground facts:

```
covers(d,a).
covers(d,c).
covers(d,b).
```

This section, explains how features and relations are encoded as Prolog facts. To represent a region-set that includes one or more regions, a Prolog list is used. The type of each region is represented by a particular primitive. For example, when only plane segmentation is applied, each region is a *plane*. However, if the segmentation algorithm can provide more primitives such as a *cylinder*, then the relation name used in Prolog will show the corresponding type. It is important that each region is denoted by a unique name or ID. As shown, there are five planar regions as the result of segmentation in Figure 4.2e. The regions shown in this figure can be represented as below, which is automatically generated as the result of segmentation.

The general form is:

```
plane(plane_ID).
```

and the instances of planes are:

```
plane(pl_001).  plane(pl_002).
plane(pl_003).  plane(pl_004).  plane(pl_005).
```

Since Regions 2, 3 and 5 form a box, this combination can be represented as below, which can be created automatically as the result of supervised training or labelling, as discussed later. There are two ways to represent a region-set belonging to a class: using the name of the class as the relation name, or using the class name as an argument. That is, the general form can be either:

```
object_class_name(region_set).
% or
class(object_class_name, region_set).
```

and in this example it will be

```
box([ pl_002, pl_003, pl_005 ]).
% or
class(box,[ pl_002, pl_003, pl_005 ]).
```

There is no significant difference between these two representations. Since we construct a binary classifier for each class, it is preferable to use the same declarations and settings for each class without changing the names of the relations. The first representation requires unique declarations and settings for each class, but is easier to read. Therefore, we use the second representation in our implementation, to save some effort, but in our explanations, we sometimes use the first notation, for clarity.

As mentioned earlier, the features are grouped into three categories: single region features, region relations and region-set features. The next section describes the representation of these features as defined for learning.

6 ALEPH and Language Specification for Learning

ALEPH is the machine learning toolkit that is mainly used in this research. A part of the result of learning the class *stairs* using ALEPH is shown below. The features and relations for a large set of images are extracted and passed to ALEPH as background knowledge. The implemented GUI is used to label 237 instances as positive examples and 656 negative examples of the object *stairs*. It is also necessary to give some constraints to ALEPH to reduce the search for the hypothesis. One of the rules constructed by ALEPH is given below. In this example, plane segmentation is used and ALEPH is compiled with SWI-Prolog.

```
%[Rule] [Pos cover = 213    Neg cover = 0]
stairs(REG_SET) :-
    member(C, REG_SET),  member(D, REG_SET),
    angle(D, C, '0 ± 15'),
    member(E, REG_SET),
    angle(E, C, '90 ± 15'),  angle(E, D, '90 ± 15'),
    distributed_along(E, axis_X).
```

This rule covers 213 positive examples (over 89.87% of total positives) and no negative examples. The *member* relation, which is predefined in Prolog, specifies that the first argument is a member of the list that is provided as the second argument. In other words, the primitive (plane) exists in the given region-set or the region belongs to the region-set.

This clause defines a region-set as belonging to the class *stairs* if it has at least three planes, C, D and E of which regions C and D are approximately parallel, both regions C and D are approximately perpendicular to region E and region E is distributed mostly along the X-axis.

In addition to providing positive and negative examples to ALEPH, some constraints on the hypothesis language must be given [24]. Mode declarations have the form:

```
mode(RecallNumber,PredicateMode).
```

The first argument, *recall number*, specifies the maximum number of instances for the predicate. This must be a positive number greater than or equal to 1 or '*', which represents no limit. For example, for predicate *parent(P, C)*, the recall number is 2 since a child can have two parents [58], while for *sister(S1, S2)*, the recall number does not have a limit.

The second argument defines how a predicate must be called. It follows the template below:

```
p(ModeType, ModeType, ...).
```

ModeTypes can be simple or structured. A simple ModeType has three possible forms: +T, -T and #T. A '+' means that the variable is treated as input of the specified type, while '-' indicates an output variable of the given type and '#' specifies that it is a constant of the given type. A structured ModeType follows the form *f(..)* where *f* is a function symbol, and its arguments may also be simple or structured ModeTypes. For example,

```
:- mode(1,mem(+number,+list)).
```

shows a mode declaration having solely simple modetypes while

```
:- mode(1,mem(+number,[+number|+list])).
```

shows an example having both.

Determination statements specify the predicates that might be used for hypothesis construction:

```
:- modeb(1,angle(+region,+region,#angle_bin)).
:- modeb(1,normal_spherical_theta(+region,#angle_bin)).
:- modeb(1,normal_spherical_phi(+region,#angle_bin)).
:- modeb(*,ratio_yz(+region,#ratio_bin)).
:- modeb(*,ratio_xz(+region,#ratio_bin)).
:- modeb(*,ratio_xy(+region,#ratio_bin)).
:- modeb(*,ch_ratio(+region,#ratio_bin)).
:- modeb(*,dr_xy(+region,+region,#direction)).
:- modeb(*,dr_xz(+region,+region,#direction)).
:- modeb(*,distributed_along(+region,#axis)).
:- modeb(*,obb_ratio23(+region,#ratio_bin)).
:- modeb(*,obb_ratio13(+region,#ratio_bin)).
:- modeb(*,obb_ratio12(+region,#ratio_bin)).
:- modeb(1,rel_dif_nv_alpha(+region,+region,#angle_bin)).
:- modeb(1,rel_dif_nv_phi(+region,+region,#angle_bin)).
:- modeb(1,rel_dif_nv_theta(+region,+region,#angle_bin)).
:- modeb(1,rs_obb_ratio23(+region_set,#ratio_bin)).
:- modeb(1,rs_obb_ratio13(+region_set,#ratio_bin)).
:- modeb(1,rs_obb_ratio12(+region_set,#ratio_bin)).
:- commutative(angle/3).
:- commutative(rel_dif_nv_alpha/3).
```

Figure 6.1: Mode declarations corresponding to the features used in this research

```
determination(TargetName/Arity,BackgroundName/Arity).
```

The first argument specifies the name and arity of the target predicate, which appears in the head of the hypothesis clauses. The next argument defines name and arity of a predicate which can contribute in the body of such clauses. Only one target predicate can be used.

The features were discussed in previous sections. Next, we introduce a specification that can be used to guide our object classification method using ALEPH. Each region-set includes some regions and each region has some attributes. In addition, each region pair and each region-set might have some relations. Therefore, the following are declared:

```
:- modeb(*,n_of_parts(+region_set,#n)).
```

which directs the learning algorithm to consider the number of regions in the region-set.

```
:- modeb(*,member(-region,+region_set)).
```

which selects each region in the region-set for further processing. Other features can be declared as Figure 6.1, where the relations *angle* and *rel_dif_nv_alpha* are commutative.

For the hypothesis mode declaration, there are two possible approaches, as discussed in Section 5:

- Defining a different mode for each object class:

```
:- modeh(*,box(+region_set)).
:- modeh(*,stairs(+region_set)).
```

```
%...
:- modeh(*,wall(+region_set)).
```

- Defining a single mode with the class name as an argument:

```
:- modeh(*,class(#class_name,+region_set)).
class_name(box).
class_name(stairs).
%...
class_name(wall).
```

Similar to the previous example, an appropriate *determination* must be provided based on the above modes:

```
:- determination(box/1,angle/3). % for each object class
```

and when using the second approach for hypothesis mode declaration:

```
:- determination(class/2,angle/3).
```

Some constant definitions are also required as below:

```
                        %--- Axes ---
axis(axis_X). axis(axis_Y). axis(axis_Z).

                      %--- directions ---

direction(north).  direction(east).
direction(south).  direction(west).
direction(is_covered).  direction(covers).
direction(connected).

                      %--- angle_bins ---

anglebin('0 ± 15').  anglebin('-0 ± 15').
%...
anglebin('180 ± 15').  anglebin('-180 ± 15').
anglebin('22.5 ± 15').  anglebin('-22.5 ± 15').
%...
anglebin('157.5 ± 15').  anglebin('-157.5 ± 15').

                      %--- ratio_bins ---

ratiobin('1.0 ± 0.25').  ratiobin('-1.0 ± 0.25').
ratiobin('1.5 ± 0.25').  ratiobin('-1.5 ± 0.25').
%...
ratiobin('10.0 ± 0.25').  ratiobin('-10.0 ± 0.25').
ratiobin('10.5 ± 0.25').  ratiobin('-10.5 ± 0.25').
```

Parameter Settings in ALEPH

Some parameter settings used in ALEPH [24] are required:

- The number of literals for an acceptable clause can be limited using the following the parameter setting. The default value is 4. It is set to a higher value, 10.

```
:- set(clauselength,+V).
```

- As the dataset contains noise, experiments vary ALEPH's tolerance to noise using the following directive. The default value for V is 0, i.e. no noise.

```
:- set(noise,+V).
```

- Another parameter is an upper bound for the number of nodes for exploration during the search. The default value is 5000. A higher value of 10000 is used here and can be set by:

```
:- set(nodes,+V).
```

- Each clause covers some positive examples. However, it is possible to specify the minimum number to reject clauses with a small coverage. The default value is 1.

```
:- set(minpos,+V).
```

7 Additional Experimental Evaluation

7.1 Feature evaluation

An RGB-D dataset of some common household objects is provided by Lai et al. [29] using a Microsoft Xbox Kinect sensor. Only one object on a turntable appears in each scene. As a result, after applying segmentation to the input scene, there is no need to select which regions form an object, since most regions participate. We have performed some experiments using this dataset in our previous work [18].

Although the dataset includes 51 classes, only a subset has been chosen, including *ball*, *bowl*, *cap*, *cereal box* and *coffee mug*. Note that each class has a different number of *physically distinct instance sets*. A physically distinct instance set (PDIS) is a collection of images of a particular instance of a class taken from different angles by rotating the object on a turntable and from different camera mounting points. Using the original captured and cropped images, sub-samples are taken from each sequence for each object, taking every i_{th} frame. There is a specific split arrangement for training/testing data. Data for each object class come from a different physically distinct instance each of which is stored separately. For example, data for the class *ball* are saved in 7 folders, while the number of folders for the *bowl* object class is 6. As suggested by Bo et al. [59], for each iteration of learning, one PDIS of each object is chosen randomly as the test set and the rest form the training set. This random train/test split technique is k-fold cross validation, with a specific implementation to test the classification on a PDIS of an object which has not been used for training.

Table 7.1: Numerical information about the chosen subset of RGB-D dataset used as the first dataset

Object class	Pos#	Neg#	PDIS#	Number of images for each PDIS
ball	225	582	7	[33,32,33,32,32,32,31]
bowl	160	647	6	[24,24,24,23,33,32]
cap	104	703	4	[26,27,25,26]
cereal box	119	688	5	[23,25,25,24,22]
coffee mug	199	608	8	[22,23,23,22,22,22,33,32]
Total	807			
PDIS#: Number of physically distinct instance sets				

We refer to this implementation as *folder-based split*. For each class, the chosen physically distinct instance sets for training are treated as positive or negative examples for training based on the current object, while the union of test sets is used for testing for all objects.

In this section, experiments are conducted on a subset of this RGB-D dataset with different configurations. The aim is to measure learning performance using only plane segmentation on household objects that have curved surfaces. The distance threshold option is used. The experiments seek to test some features not covered in the previous experiments:

- *Region-set oriented bounding box and its ratios* (Section 4.3.2). This feature is added to set to the basic configuration to determine how it affects the performance.
- *Relative difference between normals* (Section 4.2.3) instead of *directional relationship* features.
- Using each region's *oriented bounding box* features (Section 4.1.4) instead of its *bounding box* features.
- Combine two of the above new features.

The configurations for this set of experiments are presented as in Figure 7.1. There are five configurations using five classes from the RGB-D dataset based on a sub-sampling factor of 25. Since the objects in the RGB-D dataset are much smaller when compared to the planar objects previously used, the minimum size for a region to be accepted is decreased by setting *min_region_size_base*=10.

The number of physically distinct instance sets for each class, the number of images in each PDIS and the number of positive and negative examples used for this experiment set are presented in Table 7.1.

As mentioned earlier, the folder-based split approach is used for this experiment set. Table 7.2 shows the performance comparison for the configurations used including the number of rules and the compression average. The measures are provided per configuration in the form of the weighted mean and standard deviation values. The results show that:

% method:
PLOCRL (*PLane-based Object Categorisation using Relational Learning*)

% segmentation method used: just plane segmentation

```
% minimum region size: decreased.
% angle threshold: 20°
% distance threshold: used
:- set(noise,10).
% data: RGB-D dataset using every 25th frame

    % ball, bowl, cap, cereal box, coffee mug

% features common between all configurations

    % angle
    % normal_spherical_theta, normal_spherical_phi
    % ch_ratio

% additional features for configuration(1)

    % ratio_yz, ratio_xz, ratio_xy, distributed_along
    % dr_xy, dr_xz

% additional features for configuration(2)

    % ratio_yz, ratio_xz, ratio_xy, distributed_along
    % dr_xy, dr_xz
    % rs_ratio_obb23, rs_ratio_obb13
    % rs_ratio_obb12

% additional features for configuration(3),
(testing dr versus rel_dif_nv)

    % ratio_yz, ratio_xz, ratio_xy, distributed_along
    % rel_dif_nv_alpha
    % rel_dif_nv_phi
    % rel_dif_nv_theta

% additional features for configuration(4),
(testing BB versus OBB)

    % obb_ratio23
    % obb_ratio13
    % obb_ratio12
    % dr_xy, dr_xz

% additional features for configuration(5),
(using both OBB and rel_dif_nv)

    % obb_ratio23
    % obb_ratio13
    % obb_ratio12
    % rel_dif_nv_alpha
    % rel_dif_nv_phi
    % rel_dif_nv_theta
```

Figure 7.1: Configurations for experiments involving the RGB-D dataset

Table 7.2: Comparing overall weighted mean and the standard deviation for feature evaluation experiments

Experiment	Accuracy (%)	Precision (%)	Recall (%)	Number of Rules	Compression Average
1	**89.21±2.88**	**70.47±4.24**	**76.97±7.82**	**11.79±0.78**	**16.44±1.50**
2	88.71±2.91	68.64±5.21	76.66±6.47	12.96±1.18	15.17±1.30
3	89.29±2.99	69.97±5.60	77.26±7.69	11.99±0.40	15.45±1.45
4	87.79±2.55	67.43±3.82	74.67±7.26	11.12±0.65	15.38±1.06
5	**90.84±2.25**	**73.52±3.06**	**81.92±7.96**	**10.13±0.62**	**19.65±2.05**

Experiment 1 :	No feature substitution
Experiment 2 :	Adding oriented bounding box ratios for region-set
Experiment 3 :	Directional relationships versus relative difference between normals
Experiment 4 :	Bounding Box versus Oriented Bounding Box for each region
Experiment 5 :	Combination of 3 & 4

- Using the region-set oriented bounding box feature has no major effect on overall measures at least for the selected object classes.
- The alternative features (using *relative difference between normals* instead of *directional relationships* and the *region's oriented bounding box* instead of *bounding box*) are practical and even their substitution combination increases the performance and average compression, as well as reducing the number of rules.

In addition to the overall measures, it is useful to examine the performance measures per class as shown in Table 7.3. The results show that:

- Accuracy, precision and recall are improved after each single substitution (Configurations 3 and 4) more than 40% of the time.
- Comparing the basic configuration (configuration 1) and combined substitution configuration (configuration 5), the accuracy, precision and recall are improved 80%, 60% and 80% of the time respectively, which suggests the benefits of using these substitutions together.
- Accuracy, precision and recall are improved for the class *cap* after using the *region-set bounding box ratio* feature, which shows its potential for further investigation.

Regarding the number of rules and compression average:

- Improvement is obtained more than 60% of the time by any single feature substitution.
- Comparing the basic configuration (configuration 1) and combined substitution configuration (configuration 5), 80% of the combined substitutions have fewer rules with a greater compression average.

Table 7.3: Comparing each object class weighted mean and the standard deviation for feature evaluation experiments

Object	Experiment	Accuracy (%)	Precision (%)	Recall (%)	Number of Rules	Compression Average
ball	1	**88.39±3.16**	**73.65±9.64**	**85.27±10.53**	**11.89±1.50**	**26.55±2.78**
	2	88.39±3.16	72.87±6.85	84.87±10.48	12.22±2.23	26.91±3.96
	3	87.27±2.82	70.64±6.63	82.04±6.55	13.44±1.97	21.38±3.43
	4	85.03±2.23	66.15±6.32	79.7±11.44	11.11±2.17	24.55±3.97
	5	**87.42±2.64**	**69.13±6.16**	**87.35±7.81**	**10.56±1.40**	**29.2±1.93**
bowl	1	**85.32±4.24**	**65.33±11.61**	**62.62±25.15**	**11.67±1.89**	**12.38±1.61**
	2	84.13±3.31	59.86±12.72	63.09±30.56	11.89±2.59	11.58±1.80
	3	84.58±4.79	62.62±11.95	60.53±29.29	11.44±1.61	14.41±3.16
	4	82.7±5.29	56.37±12.56	57.19±26.07	10.33±1.79	12.47±2.88
	5	**85.55±4.12**	**63.6±8.06**	**65.39±27.49**	**10.89±2.04**	**12.47±2.10**
cap	1	**88.02±3.31**	**69.47±8.83**	**70.13±11.22**	**6.89±0.96**	**12.44±2.02**
	2	88.62±3.31	71.96±8.60	70.74±10.39	10.00±1.41	7.69±2.09
	3	88.02±2.82	70.09±8.60	70.31±7.87	7.56±1.39	8.69±1.72
	4	89.14±4.24	73.15±12.04	69.66±15.19	6.11±1.26	12.85±3.10
	5	**94.9±2.44**	**86.71±9.05**	**88.85±4.12**	**6.11±1.17**	**19.17±4.38**
cereal box	1	**97.38±1.73**	**91.9±8.12**	**94.09±7.07**	**3.44±0.48**	**35.8±5.09**
	2	96.55±2.23	88.73±9.00	93.33±6.40	3.78±0.65	35.24±5.67
	3	96.78±1.73	89.41±6.78	93.31±6.16	4±0.82	31.49±4.21
	4	97.67±1.41	93.2±5.74	94.06±9.11	3.11±0.85	40.93±10.08
	5	**97.67±1.41**	**93.5±3.74**	**93.26±8.94**	**3.78±0.8**	**34.24±7.33**
coffee mug	1	**78.44±4.58**	**45.44±8.94**	**65.16±13.96**	**17.44±3.03**	**8.42±1.68**
	2	77.47±4.79	43.83±8.42	64.24±11.31	18.56±3.34	8.1±1.14
	3	81.06±5.19	49.96±8.71	72.42±15.96	15.78±2.68	8.78±2.75
	4	75.82±3.31	41.44±7.48	64.92±5.74	17.78±2.90	6.47±1.11
	5	**79.86±3.00**	**47.65±6.48**	**66.9±18.22**	**12.78±2.68**	**11.32±2.28**

Experiment 1 : No feature substitution

Experiment 2 : Adding oriented bounding box ratios for region-set

Experiment 3 : Directional relationships versus relative difference between normals

Experiment 4 : Bounding Box versus Oriented Bounding Box for each region

Experiment 5 : Combination of 3 & 4

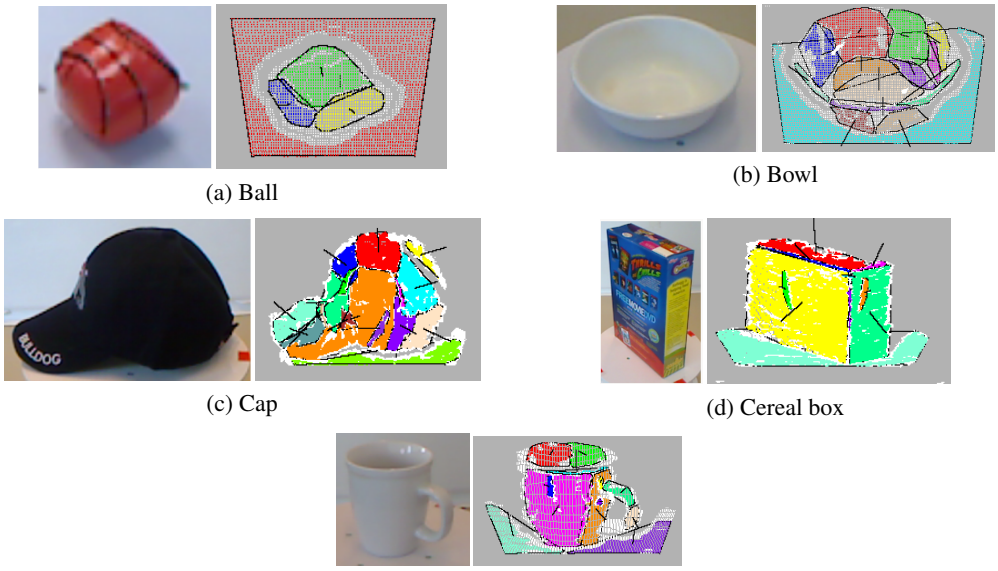

(a) Ball

(b) Bowl

(c) Cap

(d) Cereal box

(e) Coffee mug

Figure 7.2: Colour and segmented version of selected objects from the RGB-D dataset

Because only *plane* primitives have been used, lower accuracy might be expected for this experiment in comparison to previous experiments in which objects with mostly planar surfaces were used [16, 17, 18]. However, the high accuracy obtained in the above experiments shows that the method can be applied to an object with curved surfaces. However, rules are expected to be larger, with less compression. Thus, extending segmentation to cover more primitive shapes such as cylinders and spheres might lead to an improvement in accuracy, but particularly should result in rules that are more readable and may be learned more quickly. More regions should be expected when using only plane segmentation. Figure 7.2 shows an example for each class after segmentation in which each region is represented by its convex hull. Extending the segmentation should decrease the number of extracted regions as well as leading to less complexity for learning.

7.2 Comparison with a Non-Relational Object Classifier

As discussed in our previous work [18], Bo et al. [59] present a non-relational object classifier using an RGB-D dataset [29] with promising accuracy. Their method is compared with the method developed in this research, PLOCRL, using folder-based split approach as previously described. Bo et al. [59] provide MATLAB code[3] for comparison. However, at the time of this experiment, a modification of the classification method was needed following the documentation provided in their C++ code, which meant using the 'linear' option to scale the training and testing data. They introduced depth kernel descriptors for classification using depth and colour images. However, since the current research uses solely range data, and their corresponding point clouds, the related gradient kernel descriptors (*Gradient KDES*), local binary pattern kernel descriptors (*LBP KDES*), dense normal kernel descriptors (*Normal KDES*), size kernel descriptors (*Size KDES*), and their combinations are used for comparison.

[3] http://www.cs.washington.edu/ai/Mobile_Robotics/projects/kdes/

Table 7.4: Numerical information about the chosen subset of RGB-D dataset used as the second dataset

Object class	Pos#	Neg#	PDIS#	Number of images for each PDIS
ball	225	761	7	[33,32,33,32,32,32,31]
bowl	160	826	6	[24,24,24,23,33,32]
cap	104	882	4	[26,27,25,26]
cereal box	119	867	5	[23,25,25,24,22]
coffee mug	199	787	8	[22,23,23,22,22,22,33,32]
sponge (planar)	179	807	6	[26,24,32,33,31,33]
Total	986			
PDIS#: Number of physically distinct instance sets				

Table 7.5: Numerical information about the chosen subset of RGB-D dataset used as the third dataset

Object class	Pos#	Neg#	PDIS#	Number of images for each PDIS
ball	225	889	7	[33,32,33,32,32,32,31]
bowl	160	954	6	[24,24,24,23,33,32]
cap	104	1010	4	[26,27,25,26]
cereal box	119	995	5	[23,25,25,24,22]
coffee mug	199	915	8	[22,23,23,22,22,22,33,32]
sponge (total)	307	807	10	[26,24,32,33,31,33,32,32,32,32]
Total	1114			
PDIS#: Number of physically distinct instance sets				

Three datasets are used for this comparison. One dataset includes five classes used in the previous section (*ball*, *bowl*, *cap*, *cereal box*, *coffee mug*) taking every 25th image from the image sequence as shown in Table 7.1. For the second dataset, a subset of the class *sponge* is added, which is mostly planar with the same sampling factor (see Table 7.4). The third dataset is the second dataset plus the rest of the class *sponge*, which is not mostly planar with the same sampling factor (Table 7.5).

The PLOCRL method uses two configurations: basic and extended, which are the first and the last configurations (configurations 1 and 5 respectively) explained in the previous section, as before and after both feature substitutions. For both configurations, only plane segmentation is used. Since Bo et al. [59] give only the average accuracy of classification, this measure is used with the above descriptors to compare against this research's method, PLOCRL, for these two configurations. The results are shown in Table 7.6.

Bo et al. [59] build a multi-class classifier, while the method developed here employs a binary classifier for each object class. Therefore, the accuracy measure for our method must consider positive examples for each class, ignoring negative examples as discussed

Table 7.6: Comparing mean and the standard deviation of accuracy with a non-relational method using three subsets of the RGB-D dataset

Method	Dataset 1	Dataset 2	Dataset 3
	Accuracy	Accuracy	Accuracy
Gradient KDES	69.38±8.56	69.38±8.56	69.87±14.69
LBP KDES	65.86±14.31	68.95±8.65	71.73±13.44
Normal KDES	77.25±7.31	72.02±8.06	72.76±12.24
Size KDES	74.61±12.83	68.32±13.11	76.05±9.47
Gradient + LBP KDES	**82.53±9.60**	**74.08±12.62**	**78.98±11.60**
combination of all	**84.36±8.63**	**76.79±13.28**	**82.03±10.15**
Basic version of PLOCRL	**75.23±8.30**	**76.85±5.10**	**73.26±4.38**
Extended version of PLOCRL	**79.92±8.16**	**79.70±6.05**	**74.27±8.18**

Dataset 1: ball, bowl, cap, cereal box, coffee mug

Dataset 2: ball, bowl, cap, cereal box, coffee mug, sponge (planar)

Dataset 3: ball, bowl, cap, cereal box, coffee mug, sponge (total)

by Abudawood and Flach [60]. That is, we calculate and sum true positive values for all classes, then divide the result by the total number of positive examples used for testing to determine the accuracy of PLOCRL as a multi-class classifier. In this case, since positive examples of one class are treated as negative examples of other classes, when TP_i represents the true positive for the binary classifier for object class i, then the accuracy for the multi-class classifier using n binary classifiers is $\frac{\sum_{i=1}^{n} TP_i}{\sum_{i=1}^{n} TP_i + \sum_{i=1}^{n} FN_i}$, which is equal to $\frac{\sum_{i=1}^{n} TP_i}{N}$, where N is the total positive examples used for testing.

Although the PLOCRL method used solely planar primitives, the comparison shows that its accuracy is very close to a state-of-the-art classifier even when it is tested on a subset of common objects having curved surfaces. The PLOCRL outperforms the majority of depth kernels most of the time. While the accuracy of a non-relational object classifier decreases by adding a planar shape object to the dataset, the accuracy of PLOCRL method increases. However, as expected, due to using plane segmentation, adding non-planar object shapes affects the accuracy of the method slightly. Besides accuracy, the method inherits relational learning benefits over non-relational methods. It describes the relationship between sub-parts, which is a useful feature of relational learning. In addition, knowledge accumulation, learning by using previously learned concepts in background knowledge, is an additional superior aspect of using relational learning. These two properties are not present in other methods such as the depth kernel descriptors.

7.3 Discriminative versus Descriptive Rules

The rules induced by ALEPH are discriminative rather than descriptive. For example, a *stair*s object can be defined by a different number of regions:

```
stairs([pl_01,pl_03,pl_04,pl_05,pl_06,pl_08]).
stairs([pl_01,pl_03,pl_04,pl_05]).
```

Both form a staircase but one is a subset of the other. If the induced rule for the smaller region-set can cover the larger one, ALEPH will not generalise it. That is, ALEPH creates a rule that is sufficiently practical to discriminate, but it is not necessarily the most descriptive rule. To create a more descriptive rule, further directions must be given to ALEPH. Additional analysis of examples used for training may also be necessary.

Searching for clauses in ALEPH is affected by two parameters: the search strategy and the evaluation function. These parameters can be defined by:

```
:- set(search,Strategy).
:- set(evalfn,Evalfn).
```

where *Strategy* can be *ar*, *bf*, *df*, *heuristic*, *ibs*, *ic*, *id*, *ils*, *rls*, *scs* and *false*. For example, *bf*, which is the default strategy, enumerates shorter clauses before longer ones. *EvalFn* can take the values *coverage, compression, posonly, pbayes, accuracy, laplace, auto_m, mestimate, entropy, gini, sd, wracc,* or *user define*. Investigating the options for the search strategy and the evaluation function may be helpful to achieve rules that are more descriptive.

As shown earlier in the previous work [17, 18], learned concept descriptions can be put into background knowledge to help learn another concept description. Additionally, a concept like *stair*s can be represented by a recursive description. To achieve a recursive rule, it might be necessary to define an evaluation function that rewards a recursive rule, since a recursive rule might be ignored if another rule is considered superior with respect to the current evaluation function. However, the most important factor in achieving a recursive rule is providing appropriate mode declarations and determinations which guide ALEPH to reduce the size of input arguments in the hypothesis.

ALEPH constructs three non-recursive rules for *stair*s, using only *angle* predicates as shown in Figure 7.3.

It is also able to construct recursive rules when some help is provided in the form of a declaration to accept a hypothesis as the output rule. For the current research, it was possible to make ALEPH learn a recursive description for *stairs* by the following mode declarations and determinations. These declarations and determinations guided ALEPH to replace a plane-set with a smaller subset of itself to form a recursive description:

```
%[Rule 1] [Pos cover = 143    Neg cover = 2]

stairs(REG_SET) :-
    member(C,REG_SET), member(D,REG_SET),
    angle(D,C,'0±15'), member(E,REG_SET),
    angle(E,D,'0±15'), angle(E,C,'0±15').

%[Rule 2] [Pos cover = 213    Neg cover = 1]

stairs(REG_SET) :-
    member(C,REG_SET), member(D,REG_SET),
    angle(D,C,'0±15'), member(E,REG_SET),
    angle(E,D,'90±15'), angle(E,C,'90±15').

%[Rule 3] [Pos cover = 92    Neg cover = 0]

stairs(REG_SET) :-
    n_of_parts(REG_SET,4), member(C,REG_SET),
    member(D,REG_SET), angle(D,C,'0±15').
```

Figure 7.3: Non-recursive rules for a *stairs* object class using only *angle* predicate

```
:- mode(*,stairs(+plane_set)).
:- mode(*,member(-plane1,+plane_set)).
:- mode(*,member(-plane2,+plane_set)).
:- mode(1,angle(+plane1,+plane2,#angle_bin)).
:- mode(1,((+plane_set) = ([-plane1|-plane_set]))).
:- mode(1,((+plane_set) = ([-plane2|-plane_set]))).
:- commutative(angle/3).

:- determination(stairs/1,stairs/1).
:- determination(stairs/1,'='/1).
:- determination(stairs/1,member/2).
:- determination(stairs/1,angle/3).
```

The result is as below for a total of 237 positive examples and 656 negative examples using solely the *angle* feature:

```
[Rule 1] [Pos cover = 227    Neg cover = 8]
stairs(B) :-
    B=[C|D], D=[E|F], F=[G|H],
    member(I,D), angle(C,I,'0±15').

[Rule 2] [Pos cover = 207    Neg cover = 0]
stairs(B) :-
    B=[C|D],  stairs(D).
```

The second rule is the recursive one that accepts a region-set B as *stairs* if another plane-set D is *stairs*, while D is the remaining plane-set after removing the head *plane(s)* from the plane-set B.

In summary, ALEPH can provide rules based on relational information between primitives and features. These rules are practical enough to classify objects into different classes. However, the rules might be different from a human's description of the concept.

8 Details and Configurations

8.1 Data Gathering

8.1.1 General Procedure

As mentioned earlier, range data are captured using different depth cameras from various environments. The range images are generally saved in *pgm* or *png* formats. The range camera is mounted on a robot, which is driven into the environment, stopped where needed, and a sequence of images are taken when the robot is not moving. During each capture session, the camera is moved according to predefined pan, tilt and zoom values provided to the robot through the configuration file. To ensure a high quality image, without blurring, a user-defined value sets a delay after each camera movement and before the next shot. An example of such a setting for the server side is as below, which specifies the camera the Kinect Xbox and pan angles $-30°$, $-20°$, $-10°$, $-5°$, $0°$, $5°$, $10°$, $20°$ and $30°$ for each capture session. It also forces a 600ms delay between each shot.

```
<foreground
    type="CollectImages" PTZ="PTU"
    Cameras="DepthCam Kinect" WaitTimeMSecs="600">
    <justpandeg pan="-30" />
    <justpandeg pan="-20" />
    <justpandeg pan="-10" />
    <justpandeg pan="-5" />
    <justpandeg pan="0" />
    <justpandeg pan="5" />
    <justpandeg pan="10" />
    <justpandeg pan="20" />
    <justpandeg pan="30" />
</foreground>
```

On the GUI side, the following entry defines how the capture session is started and what task must be run. As shown, the task begins when the '*c*' key is pressed.

```
<fgtask key="c" task="CollectImages" />
```

Each snapshot must be numbered sequentially and saved in the same collection folder. Since having a colour version of scene can help the user, especially for labelling, the user has the

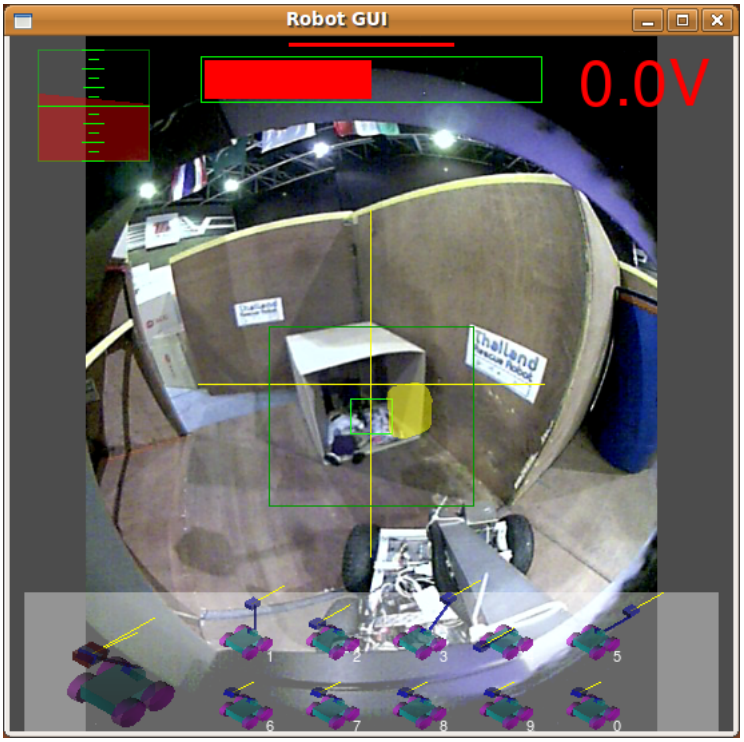

Figure 8.1: A robot panel showing a camera input

option to configure the system to take both colour and depth images for each snapshot. The colour images are generally saved in *ppm* or *png* formats. The operator of the robot is able to see the colour and depth versions of the scene through a panel before starting the capture process. Figure 8.1 shows the panel window that displays the state of the robot and the scene in front of the robot. The user can control the robot arm that carries the cameras by choosing pre-defined positions or by using the keyboard to set the desired angle before starting image collection.

8.1.2 Using Other Image Collection Systems

The image collection module used in this research applies to all range cameras: the SwissRanger SR3000, Kinect Xbox and ASUS Xtion Pro Live. However, NiViewer, a tool in the OpenNI[4] toolkit developed by PrimeSense[5], can also be used to capture image with the ASUS Xtion Pro Live, although the output of this program has different format. Hence, we implemented a small program to convert this output into the same format as the rest of the image collection module.

8.1.3 Image Collection Without Using a Robot

The image collection module does not have to be run on a robot. It can be run on a computer connected to a range camera. In this case, there is no option to move the camera around and only one image per capture session can be taken. The user can move the camera or the object manually to cover different views.

[4] http://www.openni.org/
[5] http://www.primesense.com/

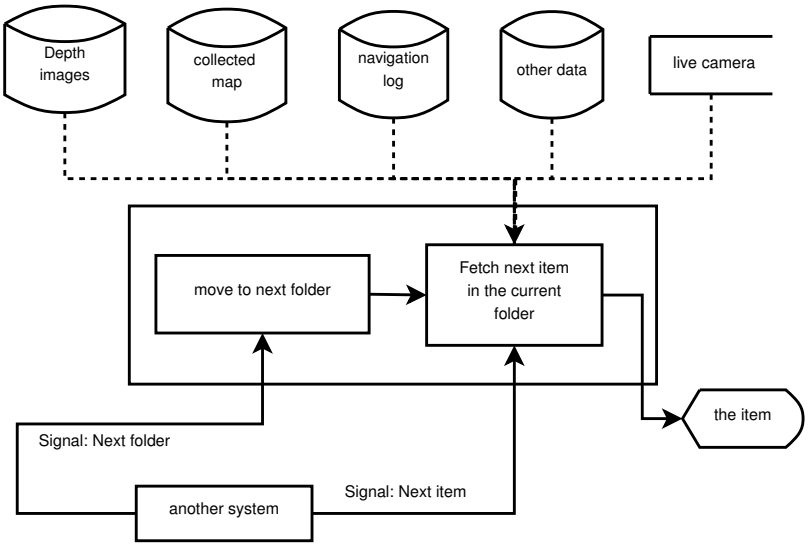

Figure 8.2: Illustration of the module developed for fetching data from folders/sub-folders

8.2 Pre-processing, Feature Extraction and Labelling

8.2.1 From Range Image to Point Cloud

Range images are stored in folder and sub-folder structure. For example, a folder named *stairs* can contain some sub-folders. Images related to this object class are placed in each sub-folder. This facilitates folder-based split implementation, which splits objects into training and test sets and eliminating one specific instance set from the training set to put it in the test set. For most perception and learning tasks, point clouds are created from range images. These can be sampled, sub-sampled and converted to other formats such as the PCL's point cloud format, known as Point Cloud Data (PCD)[6].

8.2.2 Fetching Input Data

A module is implemented to navigate each folder and its sub-folders and to fetch one item at each step as shown in Figure 8.2. This module can ignore the rest of the items in the sub-folder and jump to the next sub-folder based on a user request. It can create a dynamic naming based on the current item that can be used later in other modules such as segmentation results and labelling. If the item is a range image and a corresponding masked image is provided to separate the desired object from the background in the range image, such as the RGB-D dataset provided by Lai et al. [29], this module is able to apply this mask, creating a masked version of the range image for further processing.

For example, the entry below in the configuration file defines such a navigation scenario for the system to fetch range images. The configuration defines how to fetch input images with the following parameters:

- one folder or all sub-folders
- folder, name pattern, file sampling factor

[6] http://pointclouds.org/documentation/tutorials/pcd_file_format.php

- point cloud sampling factor
- cropped or full image? what is the original frame for the cropped version?
- other files attached such as colour and masking
- training action: automatic Positive/Negative examples or defined by user

```
<background name="navigateObjSSList">
<Collection

    name="ball" filetype="*_depthcrop.png"
    dir="./rgbd-dataset/cropped/rgbd-dataset/ball/"
    use_layerNaming="false" fileStep="5"
    num_deleted_prefix="0" num_deleted_suffix="14"
    action="POS" add_to_prefix="" add_to_suffix=""
    depthCam="KinectNew" ystep="1" xstep="1">
    <putToFrame w="640" h="480"/>
    <otherfiles id="colour"
        add_to_prefix="" add_to_suffix="_crop.png"/>
    <otherfiles id="mask"
        add_to_prefix="" add_to_suffix="_maskcrop.png"/>
    <otherfiles id="location"
        add_to_prefix="" add_to_suffix="_loc.txt"/>
</Collection>
...
<Collection
...// another collection of input images
</Collection>
</background>
```

In this example, the instances of the class *ball* are stored in a nested folder structure starting from the specified directory. The name of each range image follows a pattern shown as '*_depthcrop.png' and every fifth image is selected. The camera is a Kinect and the sampling rate for the point cloud must not be applied. For labelling, every image must be treated as a positive example and the user does not need to interfere. Since the image is cropped, the original frame dimensions are provided here as well. In addition to the range image, colour image and masking image files are provided. Another file, location, defines the top-left corner coordinate of the object in the scene. The names of additional files follow the input pattern of the range image by removing and adding prefixes and suffixes as specified. That is, if the name of an input image is 'X_depthcrop.png', the corresponding colour image, masking image and location images are 'X_crop.png', 'X_maskcrop.png' and 'X_loc.txt' respectively.

This module is extended to work with any logged range data, such as maps and navigation logs, where there is no one-to-one correspondence between sensor data due to their different capture rates. This module also is able to fetch any other type of input to pass it

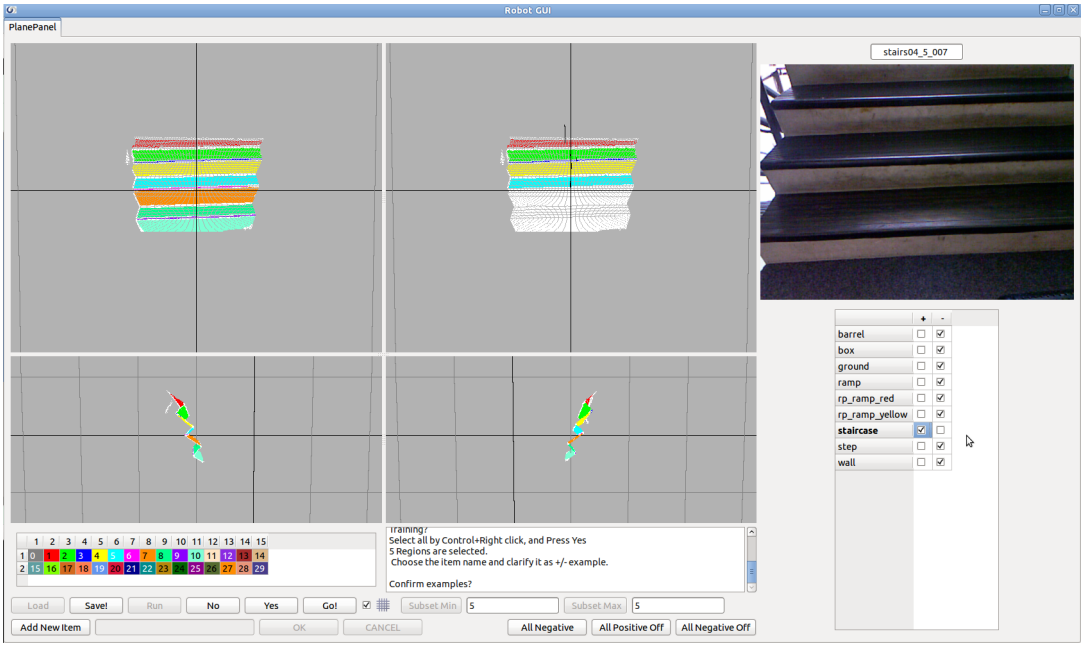

Figure 8.3: An example of labelling process by using the GUI. Top-right view shows the selected regions.

to the next component in the system. This capability is used to load already segmented data for the feature extraction module.

After loading a range image, if the user does not want to ignore it or in the case of automatic processing, the image is passed to another module to be converted to a point cloud. For this purpose, it is important to know the specification of the camera originally used for image capture. This information is provided in the input configuration file for each batch of input images.

Since a corresponding point cloud can have many points, making processing time consuming, the user can specify a sampling factor to control the point cloud resolution. There are different methods for sampling a point cloud [61]. However the easiest is to take every i_{th} point based on the range image's 2D grid, which is possible when the point cloud is ordered. Note that i is the sampling rate.

8.3 Labelling

Labelling can be manual or automatic. For manual labelling, the visual output of segmentation is provided to the user via the GUI. Each region is coloured differently to make it easier for the user to select. The user can click on any point of a region to add the region to the current region-set. After adding all desired regions to the region-set, the user can specify how the training example must be treated: a positive example for one specific class and negative example for some classes. An example of the GUI is shown in Figure 8.3.

An object class can be defined by various number of regions. For example, as shown in Figure 8.4, a *staircase* can be formed by 4, 5, 6 and 7 segmented planes. It is time-consuming for the user to select all 4, 5, 6 and 7 combinations of such planes manually. Therefore, optional values are added to define the minimum and maximum number of re-

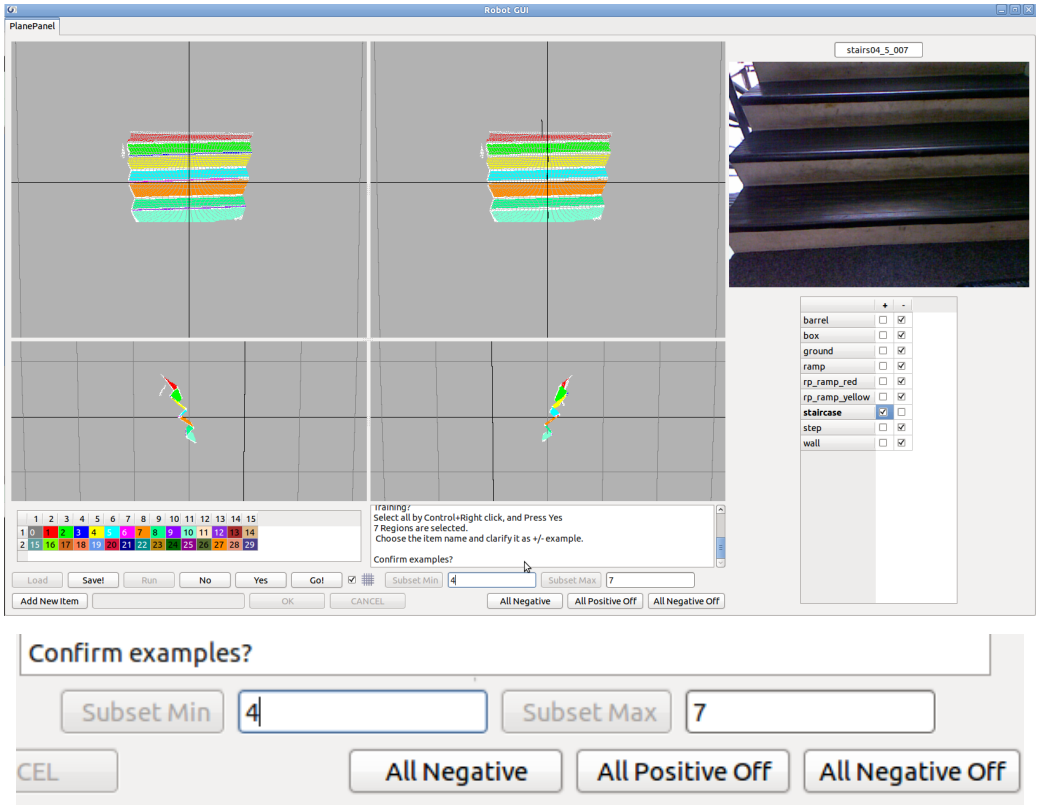

Figure 8.4: Setting the minimum and maximum region-set size in the GUI to produce more than one region-set during manual labelling

gions forming an object. Figure 8.4 shows a situation where the user has selected seven regions such as p_1, p_2, p_3, $p_{4,}$, p_5, p_6 and p_7, but aims to form objects containing four to seven regions and labels each as a *staircase*. By using four as the minimum and seven as the maximum, any four to seven sub-lists of the above regions will be automatically labelled as an instance of *staircase*. That is, the region-sets below will be created:

$\{p_1, p_2, p_3, p_4\}$, $\{p_2, p_3, p_4, p_5\}$, $\{p_3, p_4, p_5, p_6,\}$, $\{p_4, p_5, p_6, p_7\}$,
$\{p_1, p_2, p_3, p_4,, p_5\}$, $\{p_2, p_3, p_4, p_5,, p_6\}$, $\{p_3, p_4, p_5, p_6,, p_7\}$,
$\{p_1, p_2, p_3, p_4,, p_5, p_6\}$, $\{p_2, p_3, p_4,, p_5, p_6, p_7\}$ and
$\{p_1, p_2, p_3, p_4,, p_5, p_6, p_7\}$

In the case of automatic labelling, all regions from the segmentation module will form a region-set and an instance of an object class. Depending on the input configuration, the segmentation result will be saved as a positive example for the specified class and as negative examples for the other classes. If automatic labelling is activated, but the type of example (positive or negative) has not been provided, the region-set will be shown in the user interface and the user will specify the type of region-set through the interface.

8.4 Configuration File for the Main Processing Module

A configuration file must be provided for the main pre-processing component. It sets the values for the parameters such as:

- The type of the camera producing the images
- The control panel for the main system (plane segmentation and feature extraction):
  - ◇ camera density
  - ◇ using logger option
  - ◇ using normal smoothing option
  - ◇ the option of angle criterion for the segmentation
  - ◇ activating step by step confirmation for processing
  - ◇ number of views used for point cloud visualisation
  - ◇ choosing the regions mode to be displayed: planes, cubes, oriented bounding box, convex hull, etc.
  - ◇ running mode: normal, just training, just extracting, automatic extraction and training
  - ◇ using distance threshold by calculating mesh threshold
  - ◇ create triangular mesh for the point cloud
  - ◇ save the point cloud as a PCD file
  - ◇ log the range image: when the original range image is not visible
  - ◇ base for minimum acceptable region size
  - ◇ angle threshold for segmentation
  - ◇ data fetching task: file navigation, map navigation, etc.
  - ◇ the option to save the result of segmentation as convex hulls and OBBs
  - ◇ the option to save each region points as a separate point cloud in PCD format
- Training panel:
  - ◇ the list specifies the name of the classes for training
    - □ a space separated list
    - □ a file contains the name of the object classes per line
  - ◇ training options: positive/negative
- Colour legend
  - ◇ number of rows
  - ◇ number of columns
  - ◇ height and width of legend cells

Figure 8.5 shows an example of a configuration file to control the GUI and the main process. This configuration defines a panel that specifies camera settings as a Kinect with a camera density of 10. It sets the GUI to show and store the result of segmentation visualisation

```
<gui>
<tabs>

    <tab name="PlanePanel"> <planepanel
        robot="Emu" camDensity="10.0"
        askForProcess="true" numOfViews="4"
        showRegionsModes="ConvexHulls OBBs_gottschalk"
        Training="true" Extracting="true"
        Smoothing="true" sleepTime="500000"
        calc_mesh_threhsold="true"
        logPointCloudAsPCD="false"
        convertPCDframe="false"
        min_region_size_base="10"
        angle_threshold="20.0"
        RunMode="Extract_AutoTrain"
        Task="navigateObjSSList"
        saveConvexhOBB="true"
        saveRegionsAsPCD="true">
    <Render1 z="1.5" />
    <Render2 z="2.5" y="1.5" />
    <Render3 z="2.5" x="-1.0" />
    <Render4 z="2.5" x="1.0" />
    <Legend rows="2" cols="15" row_height="20" col_width="25"/>
    <ItemPosNegSelect
        row_height="25" col_width="30" sort_items="true"
        items="ball bowl cap coffee_mug sponge"
        item_options="+ -"/>

</tabs>
</gui>
```

Figure 8.5: An example of a configuration file to control the GUI and the main process

as convex hulls and OBBs. It sets a smoothing option for normal vectors as true, and also uses distance threshold by calculation in the segmentation process. It deactivates the option of saving the point cloud in PCD format. It sets a minimum region size and angle threshold based on provided values and runs the main system in the mode of extracting and automatic labelling. Following running mode, the background task that fetches the input data is introduced. Such a task was shown in Section 8.2.2. After defining the settings for main processing, four views are defined for the points of view that the user prefers such as front, top, left and right views. The next entry defines the colour legend and finally the items to be shown in the training panel are specified, which in this case are five class labels.

Figure 8.3 has four views, a legend colour having two rows and fifteen columns and other control and monitoring options at the time of labelling five planes to form a positive example of a *staircase* and a negative example for other object classes shown in the list.

The above configuration specifies that the result of segmentation must be stored as separate regions as PCD files, which can be visualised using *pcd_viewer*[7]. It also enforces the convex hull and OBB representations of regions must be saved. Figure 8.6 shows the structure of such an output for each image.

[7] http://pointclouds.org/documentation/overview/visualization.php

```
object_name    number of regions after segmentation
region number (starts from 1)
mass of region
normal vector
number of points forming oriented bounding box (it must be 8)
point 1 of OBB
point 2 of OBB
point 3 of OBB
...
point 8 of OBB
number of points forming the boundary convex hull (let say c)
point 1 of convex hull
point 2 of convex hull
point 3 of convex hull
...
point c of convex hull
next region number ...
```

Figure 8.6: The structure of segmentation result containing regions' mass, normal, convex hull and OBB representations

8.5 Learning and Evaluation

8.5.1 Preparation

The outputs from feature extraction and labelling are saved as Prolog predicates. These predicates are appended to a file called '*features.b*', which forms the background knowledge used for learning.

Positive examples of each class are saved in a file '*X.f*' as ground facts, where X is the name of the class. Similarly, negative examples of class X are saved in file '*X.n*'. This file naming system follows the ALEPH convention for input file names.

Two implementations of k-fold cross validation are used for evaluation and separating examples into training and test sets. For the first implementation of k-fold cross validation, we use Perl scripts provided by Michael Bain. All positive examples are put together and split k-fold. One of these *k folds* is selected for testing in each iteration. This is the same selection method for negative examples.

The second method is slightly different and instances of each class are provided as different physically distinct sets. The RGB-D dataset has this attribute. Considering an experiment on objects *ball*, *bowl*, *cap*, *coffee mug* and *sponge* with 7, 6, 4, 8 and 10 physically distinct sets respectively, examples of the *ball* class are stored in seven folders, and each folder contains different views of the same physically distinct *ball* instance. That is the second implementation of k-fold cross validation, the random folder-based split, which keeps one randomly selected physically distinct set every time for testing and uses the rest for training. Unix shell scripts for this implementation of k-fold cross validation is written during this research. Table 8.1 shows the ten random folder-based split configuration used for the same experiment. For each trial, one physically distinct instance set of each object class is chosen for testing as shown in this table and the rest are used for training. That

Table 8.1: An example of the ten random folder-based split configuration

Object class	PDIS#	T_1	T_2	T_3	T_4	T_5	T_6	T_7	T_8	T_9	T_{10}
ball	**7**	1	2	3	4	5	6	7	2	4	6
bowl	**6**	2	3	4	5	6	1	2	5	3	1
cap	**4**	3	4	1	2	3	4	1	2	3	4
coffee mug	**8**	5	6	7	8	1	2	3	4	1	7
sponge	**10**	8	9	6	5	2	1	4	3	10	7
T_i: $Trial_i$											
PDIS#:	Number of physically distinct instance sets										

is, in the first trial, physically distinct sets 2, 3, 4, 5, 6 and 7 of the class *ball* are used for training, as positive examples for this class and negative examples for other classes. A physically distinct set 1 of the class *ball* is used for positive examples for testing this class and physically distinct sets 2, 3, 5 and 8 of the object classes *bowl*, *cap*, *coffee mug* and *sponge* respectively are used as negative examples for testing the class *ball*. Similarly, physically distinct sets of classes *bowl*, *cap*, *coffee mug* and *sponge* that are not used for this test, are used as training negative examples for the learning class *ball*.

Shell script for random folder-based split

The following shell script is implemented to split the positive/negative examples for the implementation of k-fold cross validation using the random folder-based split, described above. It then calls the training module followed by the testing module to calculate performance measures such as accuracy, precision and recall.

This script can take advantage of a multi-core CPU by specifying the lower and upper bounds for trial numbers. For example, to have ten trials on a Quad-Core CPU, we can use this script with bounds (1 and 3), (4 and 6), (7 and 8) and (9 and 10).

This script also handles possible interruptions, such as power failures. That is, if something interrupts or kills the processes, resuming them can avoid redoing the majority of the processing already completed. For example, if the first core was working on the i_{th} class on trial *j* at the time of the interruption, the process is resumed from this class and trial, accepting the previous ones. This script has options such as shuffling the order of examples and using fewer negative examples, given a percentage split.

To run this script, we pass the name of the configuration file containing the proper language specification, the folder containing the positive and negative examples of the classes and a file containing the name of the classes and the number of PDIS for each.

Listing 1: Shell script for evaluation using random folder-based split

```
#!/bin/bash
#
# Author: Reza Farid, UNSW, Australia
# 2011-2014
# Uses train/test split based on folders used for each object class
# if split configuration file exists, it will be used, otherwise it will be generated randomly
#
# To create train.n, there are two options:
# 1) Using all negative examples based on the split
# 2) Using percentage of each category/folders of examples based on the split
bothtest=1
# if bothtest==0 means that we just test positives and not negatives
# if bothtest==1 means that negative examples will be tested as well
# if use shuffle==1 means that positive examples for training will be shuffled
runtraintest=1

split_file_name="split.txt"
train_n_temp="temp.n"
neg_percent="0.35"
use_less_neg=0
use_shuffle=0
num_of_arg=$#
if [ $num_of_arg -lt 5 ] ; then
  echo
  echo
  echo "USAGE: $(basename $0) <Spec> <data SUFFIX> <objects_folders file> <trial_lower> <trial_upper> [use less negative=0] [bothtest=1] [use shuffle=0]"
  echo
  echo
  if [ -d "class_spec" ]
  then
    echo "type as:"
    ls class_spec -l
  else
    echo  "type such as noise, noise_nodr, ..."
  fi
  echo
  echo
  exit 1
fi
if [ $num_of_arg -gt 5 ] ; then
  use_less_neg=$6
fi
if [ $num_of_arg -gt 6 ] ; then
  bothtest=$7
fi
if [ $num_of_arg -gt 7 ] ; then
  use_shuffle=$8
fi
outfolder_base="./results/results_doall_rgbd"
[ ! -d "$outfolder_base" ] && mkdir $outfolder_base

#------------------------------------ Suffix used for data
suffixParameter=$2
data_folder="data_f_n/data_f_n_"$suffixParameter
```

```
55 echo "data_folder="$data_folder
56 #------------------------------------ Object_List_File
57 obj_list_file=$3
58 i=0
59 while read line ; do
60   #echo $line
61   part1=$(echo $line | cut -d " " -f1)
62   part2=$(echo $line | cut -d " " -f2)
63   obj_classes[${i}]=$part1
64   obj_classes_folder_count[${i}]=$part2
65   i=$(($i + 1 ))
66 done < $obj_list_file
67 objc_max=$ {# obj_classes[@]}
68 # show settings
69 for (( i = 0 ; i <  $objc_max; i++ ))
70 do
71   echo ${obj_classes[${i}]} ' :: ' ${obj_classes_folder_count[${i}]} ' ↩
       physically distinct instance set'| column
72 done
73 #------------------------------------ Trial bounds
74 trial_lower=$4
75 trial_upper=$5
76
77 total_acc=0.0
78 #-------------------------------------------------------------
79 # specification
80 #-------------------------------------------------------------
81 type=$1
82 #echo enter specification filename
83 #read specfile
84 specfile="class_"$type".b"
85 specfile_addr="class_spec/"$specfile
86 #-------------------------------------------------------------
87 # extracted predicates
88 #-------------------------------------------------------------
89 #echo enter features filename
90 #read featurefile
91 featurefile="features/features_"$suffixParameter".b"
92 outfolder0=$outfolder_base"/results_"$suffixParameter
93 [ ! -d "$outfolder0" ] && mkdir $outfolder0
94 outfolder1=$outfolder0"/results_"$type
95 if [ $use_less_neg -eq 1 ]
96 then
97   outfolder1=$outfolder1"_neg_"$neg_percent
98 fi
99 for (( i = $trial_lower ; i <=  $trial_upper; i++ ))
100 do
101   [ ! -d "$outfolder1" ] && mkdir $outfolder1
102   outfolder2=$outfolder1"/trial"$i
103   [ ! -d "$outfolder2" ] && mkdir $outfolder2
104   trial_summary_file=$outfolder2/'trial_mean.txt'
105   local_split=$outfolder2/$split_file_name
106   # check if split file exists
107   if [ -f $local_split ]
108   then
109     echo 'loading '$local_split
110     sed -i "s/]=/]= /g" $local_split
111     VALUES=$(awk '/^(chosen)/{print $NF}' $local_split)
112     cnt=0
113     echo 'VALUES= '
114     for VALUE in $VALUES
```

```
115       do
116         xc[${cnt}]=$VALUE
117         echo 'chosen folder['$cnt']= '$VALUE
118         cnt=$(($cnt + 1 ))
119       done
120     else
121       echo 'making split'
122       # select one randomized folder for each class
123       for (( objc = 0 ; objc <  $objc_max; objc++ ))
124       do
125         xc_max=${obj_classes_folder_count[$objc]};
126         xc[${objc}]=$[ ( $RANDOM % $xc_max )  + 1 ]
127         echo 'chosen folder['$objc']= '${xc[$objc]}
128         echo 'chosen folder['$objc']= '${xc[$objc]} >> $local_split
129       done
130     fi
131     [ -f "$trial_summary_file" ] && rm $trial_summary_file
132     xc_acc=0.0
133     for (( objc = 0 ; objc <  $objc_max; objc++ ))
134   # for (( objc = 0 ; objc <  1; objc++ ))
135     do
136       objname=${obj_classes[$objc]}
137       echo $objname
138       outfolder=$outfolder2/$objname
139       [ ! -d "$outfolder" ] && mkdir $outfolder
140       final_processing_file=$outfolder/'rules.result'
141       # check if processing is done for the trial and the object
142       if [ -f "$final_processing_file" ]
143       then
144         echo 'process is done for '$outfolder
145       else
146         # processing the trial and the object
147         rm -rf $outfolder/*
148         echo 'processing is started for '$outfolder
149         #
150         # forming train.b
151         #
152         cat $specfile_addr $featurefile > $outfolder/train.b
153         #
154         # forming test.f & train.f
155         #
156         text_for_search='img_'$objname'_'${xc[$objc]}'_'
157         echo 'trial '$i'::object '$xc '--->' $text_for_search
158         grep "$text_for_search" $data_folder/$objname.f > $outfolder/test.f
159         if [ $use_shuffle -eq 1 ]
160         then
161           echo 'shuffle train.f'
162           grep -v "$text_for_search" $data_folder/$objname.f > $outfolder/↩
                train.f.tmp
163           shuf $outfolder/train.f.tmp > $outfolder/train.f
164           rm $outfolder/train.f.tmp
165         else
166           grep -v "$text_for_search" $data_folder/$objname.f > $outfolder/↩
                train.f
167         fi
168         #
169         # forming test.n & train.n
170         #
171         for (( other_objc = 0 ; other_objc <  $objc_max; other_objc++ ))
172         do
173         if [ $other_objc -ne $objc ]
```

```
174         then
175           other_objname=${obj_classes[$other_objc]}
176           other_text_for_search='img_'$other_objname'_'${xc[$other_objc]}'_'
177           grep "$other_text_for_search" $data_folder/$other_objname.f >> ↩
                  $outfolder/test.n
178           if [ $use_less_neg -ne 1 ]
179           then
180             #
181             # use all negative examples
182             #
183             grep -v "$other_text_for_search" $data_folder/$other_objname.f >> ↩
                    $outfolder/train.n
184           else
185             #
186             # use_less_neg
187             #
188             no_of_folders=${obj_classes_folder_count[$other_objc]}
189             picked_folder=${xc[$other_objc]}
190             for (( folder_number = 1 ; folder_number <=  $no_of_folders; ↩
                    folder_number++ ))
191             do
192             if [ $folder_number -ne $picked_folder ]
193             then
194               text_2='img_'$other_objname'_'$folder_number'_'
195               echo 'trial '$i'::neg object '$other_objname '--->' $text_2
196               grep "$text_2" $data_folder/$other_objname.f > $outfolder/↩
                      $train_n_temp
197               n_size=$(wc -l $outfolder/$train_n_temp | awk '{print $1}')
198               no_neg_for_training=$(echo "scale=0; $n_size * $neg_percent "| ↩
                      bc)
199               echo 'total neg='$n_size $TAB 'using '$no_neg_for_training | ↩
                      column
200               shuf -n $no_neg_for_training $outfolder/$train_n_temp >> ↩
                      $outfolder/train.n
201               rm $outfolder/$train_n_temp
202             fi
203               done
204           fi
205           sed -i "s/class($other_objname,/class($objname,/g" $outfolder/test.n
206             sed -i "s/class($other_objname,/class($objname,/g" $outfolder/↩
                    train.n
207         fi
208         done
209         if [ $runtraintest -eq 1 ]
210         then
211           #-------------------------------------------------------------
212           # running dotrain_test
213           #-------------------------------------------------------------
214           echo "running dotrain_test"
215           #exit
216           bash dotrain_test.sh $outfolder 'train' $bothtest
217         fi
218         rm $outfolder/*.b
219       fi
220       test_out_file=$outfolder/'test.out'
221       if [ -f "$test_out_file" ]
222       then
223         acc=$(awk '/^(Accuracy)/{print $NF}' $test_out_file)
224         echo 'test Accuracy='$acc
225         echo 'test accuracy['$objc']= '$acc >> $trial_summary_file
226       fi
```

```
227   done
228   echo "%----- calculations done." >> $trial_summary_file
229   #-------- Calculate total accuracy and mean of total for the current trial
230   if [ $runtraintest -eq 1 ]
231     then
232     bash calc_mean.sh $trial_summary_file "test accuracy" "accuracy" ↩
          $trial_summary_file
233   fi
234 done
```

Shell script for training and testing

The following shell script is the main script for the training and testing modules using the random folder-based split. It also calculates the performance measures.

Listing 2: Shell script for training/testing

```
1  #!/bin/bash
2  #
3  # Author: Reza Farid, UNSW, Australia
4  # 2011-2014
5  #
6  num_of_arg=$#
7  if [ $num_of_arg -lt 2 ] ; then
8    echo
9    echo
10   echo "USAGE: $(basename $0) <output Directory> <class name>"
11 fi
12 alephpl="aleph_rf.pl"
13 outDir=$1
14 objname=$2
15 tmpfile=$outDir/"train_tmp.pl"
16 if [ $# -gt 2 ] ; then
17   bothtest=$3
18 else
19   bothtest=0
20 fi
21 inducetype="induce"
22 #inducetype="induce_max"
23
24 mkdir $outDir/misc
25 echo  ":- compile('$alephpl')." > $tmpfile
26 echo  ":- read_all('"$outDir"/"$objname"')." >> $tmpfile
27 #bash cat_non_comment.sh aleph.config >> $tmpfile
28 #cat aleph.config >> $tmpfile
29 echo  ":- set(recordfile,'"$outDir"/misc/record.txt')." >> $tmpfile
30 echo  ":- set(goodfile,'"$outDir"/misc/good.txt')." >> $tmpfile
31 echo  ":- $inducetype." >> $tmpfile
32 echo  ":- write_rules('"$outDir"/rules.txt')." >> $tmpfile
33 echo  ":- write_rules('"$outDir"/hyp.pl')." >> $tmpfile
34 echo  ":- open('"$outDir"/test.out',write,Stestout)," >> $tmpfile
35 echo  "set_output(Stestout)," >> $tmpfile
36 echo  "write('++++++++++++++++++++++++++++'), nl," >> $tmpfile
37 echo  "write('Testing Positive Examples...'), nl," >> $tmpfile
38 echo  "write('++++++++++++++++++++++++++++'), nl," >> $tmpfile
39 echo  "test('"$outDir"/test.f',show,Tp,NPosTot)," >> $tmpfile
40 if [ $bothtest -eq 1 ];
41 then
42   echo  "write('----------------------------'), nl," >> $tmpfile
```

```
43    echo  "write('Testing Negative Examples...'), nl," >> $tmpfile
44    echo  "write('----------------------------'), nl," >> $tmpfile
45    echo  "test('"$outDir"/test.n',show,Fp,NNegTot)," >> $tmpfile
46    echo  "Fn is NPosTot - Tp," >> $tmpfile
47    echo  "Tn is NNegTot - Fp," >> $tmpfile
48    echo  "Error is ((Fp + Fn) / (NPosTot + NNegTot))," >> $tmpfile
49    echo  "Precision is (Tp / (Tp + Fp))," >> $tmpfile
50    echo  "Recall is (Tp / (Tp + Fn))," >> $tmpfile
51    echo  "write('[Test set performance]'), nl," >> $tmpfile
52    echo  "write_cmatrix([Tp,Fp,Fn,Tn]), nl," >> $tmpfile
53    echo  "format('~tStatistics~t~72|~n~n'),"  >> $tmpfile
54    echo    "write('Error     = '), write(Error), nl," >> $tmpfile
55    echo    "write('Precision = '), write(Precision), nl," >> $tmpfile
56    echo    "write('Recall    = '), write(Recall), nl, write(' (Sensitivity)')↩
          , nl," >> $tmpfile
57    echo  "write(pos(Tp,NPosTot)), nl," >> $tmpfile
58    echo  "write(neg(Fp,NNegTot)), nl," >> $tmpfile
59  else
60    echo  "Test_Accuracy is ((Tp)/(NPosTot)) ," >> $tmpfile
61    echo  "write('[Test set performance]'), nl," >> $tmpfile
62    echo    "write('Accuracy     = '), write(Test_Accuracy), nl," >> $tmpfile
63  fi
64  echo    "write('[end of test]'),"  >> $tmpfile
65  echo  "close(Stestout)." >> $tmpfile
66  echo  ":- halt." >> $tmpfile
67  echo  ""$inducetype" in progress..."
68  swipl -q -s $tmpfile > $outDir/rules.result0
69  sed -n '/theory/,/total clauses constructed/p' $outDir/rules.result0 > ↩
      $outDir/rules.result
70  #cat "$outDir".out >> $outDir.result
71  rm $outDir/rules.result0
72  #rm $tmpfile
73  echo "["$inducetype" is used]" >> $outDir/rules.result
74  sed -n '/Training set performance/,/Accuracy/p' $outDir/rules.result
75  sed -n '/Test set performance/,/end of test/p' $outDir/test.out
76  #cat $outDir/rules.result
77  rm $tmpfile
```

8.5.2 Learning

ALEPH is the ILP learner used in most experiments described in this research. It can be compiled with two different Prolog systems: YAP[8] and SWI-Prolog[9]. In this research, ALEPH is run in SWI-Prolog. Further information about using ALEPH is provided by Srinivasan [24] and Conceição [58].

Each class description learned in each iteration is saved in a separate file. The performance measures are expressed as a confusion matrix. The file includes the Prolog rule, its coverage, the positive examples covered by the rule (True Positives) and the negative examples covered by the rule (False Positives). A script converts coverage results to an HTML file and links each example with its corresponding screen snapshots after segmentation. This HTML file can facilitate matching each false positive/negative to its visual segmentation and feature boundary result for further analyses.

[8] http://www.dcc.fc.up.pt/~vsc/Yap/
[9] http://www.swi-prolog.org/

8.5.3 Analysis

Other scripts have been written to assist in the analysis of the results of learning. These scripts make it easier to work out the role of different regions in the concept description, as discussed in our previous work [18]. For the most part, the following are calculated: overall accuracy, precision, recall, number of rules and compression average per iteration. These measures are also calculated for each class over all iterations. Some scripts are also implemented to compare different scenarios of the same dataset using different configurations such as the results provided in Section 7.

9 Conclusions

In this report, we have provided the details of the original approach used in this research, which uses *planes* as the segmentation primitives. The segmentation method is discussed in detail including the use of a distance threshold. A few features are added and used for new experiments including comparison with a state-of-the-art non-relational object classifier. The details of the system architecture, learning specifications and implementation are also provided.

Acknowledgement

This research was supported by the Australian Research Council Centre of Excellence for Autonomous Systems. We would also like to thank Team CASulaty for the use of their RoboCup Rescue platform.

Note

The code, shell scripts, data and documentation will be publicly available on UNSW-CSE Robolab Server via http://robolab.ai.cse.unsw.edu.au/∼rezaf/ocrl for research purposes subject to acknowledging the source and the related publications.

Bibliography

[1] Andreas Opelt. *Generic Object Recognition*. PhD thesis, Graz University of Technology, 2006.

[2] Shrihari Vasudevan, Stefan Gächter, Viet Nguyen, and Roland Siegwart. Cognitive maps for mobile robots–an object based approach. *Robotics and Autonomous Systems (From Sensors to Human Spatial Concepts)*, 55(5):359–371, 2007.

[3] Andrew Edie Johnson. *Spin-Images: A Representation for 3-D Surface Matching*. PhD thesis, Robotics Institute, Carnegie Mellon University, Pittsburgh, PA, August 1997.

[4] Stefan Gächter, Ahad Harati, and Roland Siegwart. Structure verification toward object classification using a range camera. In *Proceedings of the Tenth International Conference on Intelligent Autonomous Systems (IAS-10)*, pages 356–363, 2008.

[5] Roger Bostelman, Hong Tsai, Raj Madhavan, and Brian Weiss. 3D range imaging for urban search and rescue robotics research. In Hong Tsai, editor, *Safety, Security and Rescue Robotics, Workshop, 2005 IEEE International*, pages 164–169, 2005.

[6] Yutaka Hirano, Christophe Garcia, Rahul Sukthankar, and Anthony Hoogs. *Industry and Object Recognition: Applications, Applied Research and Challenges*, pages 49–64. 2006.

[7] Lars-Peter Ellekilde, Shoudong Huang, Jaime Valls Miró, and Gamini Dissanayake. Dense 3D map construction for indoor search and rescue. *Journal of Field Robotics*, 24(1-2):71–89, 2007.

[8] Mark J. Micire. Evolution and field performance of a rescue robot. *Journal of Field Robotics*, 25(1-2):17–30, 2008.

[9] Yi-an Cui, Zi-xing Cai, and Lu Wang. Scene recognition for mine rescue robot localization based on vision. *Transactions of Nonferrous Metals Society of China*, 18(2):432–437, 2008.

[10] NIST. *RoboCup and AAAI Rescue Robot Competition Rules*, 2004.

[11] May Stefan, Werner Bjorn, Surmann Hartmut, and Pervolz Kai. 3D time-of-flight cameras for mobile robotics. In *Proceedings of the 2006 IEEE/RSJ International Conference on Intelligent Robots and Systems*, pages 790–795, 2006.

[12] Felix Leon Endres. *Scene Analysis from Range Data*. Master thesis, Albert-Ludwigs-University Freiburg, Faculty of Applied Sciences, 2009.

[13] Stefan Gächter. Results on range image segmentation for service robots. Technical report, Laboratoire de Systèmes Autonomes, Ecole Polytechnique Fédérale de Lausanne (EPFL), 2005.

[14] Stefan Gächter, Viet Nguyen, and Roland Siegwart. Results on range image segmentation for service robots. In *Proceedings of IEEE International Conference on Computer Vision Systems (ICVS)*, pages 53–53, 2006.

[15] Doaa Hegazy and Joachim Denzler. Generic 3D object recognition from time-of-flight images using boosted combined shape features. In Alpesh Ranchordas and Helder Araújo, editors, *Proceedings of the Fourth International Conference on Computer Vision, Theory and Applications (VISAPP)*, volume 2, pages 321–326. INSTICC Press, 2009.

[16] Reza Farid and Claude Sammut. A relational approach to plane-based object categorisation. In *Robotics Science and System (RSS) 2012 workshop on RGB-D: Advanced Reasoning with Depth Cameras*, 2012.

[17] Reza Farid and Claude Sammut. Plane-based object categorisation using relational learning. In *Online Proceedings of the 22nd International Conference on Inductive Logic Programming (ILP2012)*, 2012.

[18] Reza Farid and Claude Sammut. Plane-based object categorisation using relational learning. *Machine Learning*, 94(1):1–21, 2014.

[19] Johann Prankl, Michael Zillich, and Markus Vincze. Interactive object modelling based on piecewise planar surface patches. *Computer Vision and Image Understanding*, 117(6):718–731, 2013.

[20] Adrien Bartoli. A random sampling strategy for piecewise planar scene segmentation. *Computer Vision Image Understanding*, 105(1):42–59, 2007.

[21] Mai Xu and Maria Petrou. 3D scene interpretation by combining probability theory and logic: The tower of knowledge. *Computer Vision and Image Understanding*, 115(11):1581–1596, 2011.

[22] Roger Mohr, Luce Morin, and Enrico Grosso. Relative positioning with uncalibrated cameras. In Joseph L. Mundy and Andrew Zisserman, editors, *Geometric Invariance in Computer Vision*, pages 440–460. MIT Press, Cambridge, MA, USA, 1992.

[23] Matthew McGill, Rudino Salleh, Timothy Wiley, Adrian Ratter, Reza Farid, Claude Sammut, and Adam Milstein. Virtual reconstruction using an autonomous robot. In *Proceedings of the International Conference on Indoor Positioning and Indoor Navigation (IPIN2012)*, pages 1–8, 2012.

[24] Ashwin Srinivasan. The ALEPH Manual (Version 4 and above). Technical report, University of Oxford, 2002.

[25] Tahir Rabbani Shah. *Automatic reconstruction of industrial installations using point clouds and images*. PhD thesis, Delft University of Technology, University of Engineering and Technology, Lahore, 2006.

[26] Waleed Kadous, Raymond Sheh, and Claude Sammut. CASTER: A robot for urban search and rescue. In *Australasian Conference on Robotics and Automation*, 2005.

[27] Waleed Kadous, Raymond Sheh, and Claude Sammut. Effective user interface design for rescue robotics. In *Proceedings of the 2006 Conference on Human-Robot Interaction*, 2006.

[28] Raymond Sheh, Waleed Kadous, and Claude Sammut. On building 3D maps using a range camera: Applications to rescue robotics. Technical Report UNSW-CSE-TR-0523, UNSW, Sydney, Australia, 2006.

[29] Kevin Lai, Liefeng Bo, Xiaofeng Ren, and Dieter Fox. A large-scale hierarchical multi-view RGB-D object dataset. In *Proceedings of International Conference on Robotics and Automation (ICRA)*, 2011.

[30] Greg Turk and Marc Levoy. Zippered polygon meshes from range images. In *Proceedings of the 21st annual conference on Computer graphics and interactive techniques*, pages 311–318, New York, USA, 1994. ACM.

[31] John A. Vince. *Geometry for Computer Graphics: Formulae, Examples and Proofs*. SpringerVerlag, 2005.

[32] Michael Ian Shamos. *Computational Geometry*. PhD thesis, Yale University, 1978.

[33] Augustine Tsai, Chun.F Hsu, I-Chou Hong, and Wen-Kai Liu. Plane and boundary extraction from lidar data using clustering. In *ISPRS Technical Commission III Symposium; Photogrammetric Computer Vision and Image Analysis (PCV)*, volume 38, pages 175–179, 2010.

[34] C. Bradford Barber, David P. Dobkin, and Hannu Huhdanpaa. The quickhull algorithm for convex hulls. *ACM Transactions on Mathematical Software*, 22(4):469–483, 1996.

[35] Michael T. Goodrich and Roberto Tamassia. Computational Geometry. In *Algorithm Design: Foundations, Analysis, and Internet Examples*, chapter 12. John Wiley & Sons, Inc., 2002.

[36] Timothy M. Chan. A minimalist's implementation of the 3-D divide-and-conquer convex hull algorithm (technical report). Technical report, School of Computer Science, University of Waterloo, 2003.

[37] Tzung-Han Lin. Approximating the minimum-bounding box of a 3D model with minimum spans for flush edges. *Materials Science Forum*, 505-507:1099–1104, 2006.

[38] Alex M. Andrew. Another efficient algorithm for convex hulls in two dimensions. *Information Processing Letters*, 9(5):216–219, 1979.

[39] Sariel Har-Peled. A practical approach for computing the diameter of a point set. In *Symposium on Computational Geometry*, 2001.

[40] Michael E. Houle and Godfried T. Toussaint. Computing the width of a set. *IEEE Transactions on Pattern Analysis and Machine Intelligence*, 10(5):761–765, 1988.

[41] Godfried Toussaint. Solving geometric problems with the rotating calipers. In *Proceedings of IEEE MELECON*, 1983.

[42] Philip Schneider and David H. Eberly. *Geometric tools for computer graphics*. The Morgan Kaufmann Series in Computer Graphics. Morgan Kaufmann Publication, 2003.

[43] Stefan Gottschalk. *Collision queries using oriented bounding boxes*. PhD thesis, The University of North Carolina, 2000.

[44] James Gregson. Fitting oriented bounding boxes. Retrieved 2014-03-05, 2011.

[45] Max Egenhofer. *Reasoning about binary topological relations*, volume 525 of *Lecture Notes in Computer Science*, pages 141–160. Springer Berlin / Heidelberg, 1991.

[46] John Freeman. The modelling of spatial relations. *Computer Graphics and Image Processing*, 4(2):156–171, 1975.

[47] David A. Randell, Zhan Cui, and Anthony G. Cohn. A spatial logic based on regions and connection. In *Proceedings 3rd International Conference on Knowledge Representation and Reasoning*, 1992.

[48] Donna J. Peuquet and Zhan Ci-Xiang. An algorithm to determine the directional relationship between arbitrarily-shaped polygons in the plane. *Pattern Recognition*, 20(1):65–74, 1987.

[49] Mehmet Dönderler, Özgür Ulusoy, and Uğur Güdükbay. *A Rule-Based Approach to Represent Spatio-Temporal Relations in Video Data*, volume 1909 of *Lecture Notes in Computer Science*, pages 409–418. Springer Berlin / Heidelberg, 2000.

[50] André Borrmann, Christoph Van Treeck, and Ernst Rank. Towards a 3D spatial query language for building information models. In *Proceedings of Joint International Conference of Computing and Decision Making in Civil and Building Engineering (ICCCBE-XI)*, 2006.

[51] Stefano Berretti and Alberto Del Bimbo. Modeling spatial relationships between 3D objects. In *18th International Conference on Pattern Recognition (ICPR 2006)*, volume 1, pages 119–122, 2006.

[52] Siyka Zlatanova, Alias Abdul Rahman, and Wenzhong Shi. Topological models and frameworks for 3D spatial objects. *Computers & Geosciences*, 30(4):419–428, 2004.

[53] Claire Ellul and Muki Haklay. Requirements for Topology in 3D GIS. *Transactions in GIS*, 10(2):157–175, 2006.

[54] Tao Chen and Markus Schneider. The neighborhood configuration model: A framework to distinguish topological relationships between complex volumes. In Olga Troyer, Claudia Bauzer Medeiros, Roland Billen, Pierre Hallot, Alkis Simitsis, and Hans Mingroot, editors, *Advances in Conceptual Modeling. Recent Developments and New Directions*, volume 6999 of *Lecture Notes in Computer Science*, pages 251–260. Springer Berlin Heidelberg, 2011.

[55] Radu Bogdan Rusu and Steve Cousins. 3D is here: Point Cloud Library (PCL). In *Proceedings of IEEE International Conference on Robotics and Automation (ICRA)*, pages 1–4, 2011.

[56] Radu Bogdan Rusu, Nico Blodow, Zoltan Csaba Marton, and Michael Beetz. Aligning point cloud views using persistent feature histograms. In *IEEE/RSJ International Conference on Intelligent Robots and Systems (IROS2008)*, pages 3384–3391, Sept 2008.

[57] PCL-PFH. Point Feature Histograms (PFH) descriptors. Retrieved 2014-03-05.

[58] João Paulo Duarte Conceição. *The Aleph System Made Easy*. Integrated Master in Electrical and Computers Engineering, Faculdade de Engenharia da Universidade do Porto, 2008.

[59] Liefeng Bo, Xiaofeng Ren, and Dieter Fox. Depth kernel descriptors for object recognition. In *Proceedings of the IEEE/RSJ International Conference on Intelligent Robots and Systems (IROS)*, 2011.

[60] Tarek Abudawood and Peter Flach. *Learning Multi-class Theories in ILP*, volume 6489 of *Lecture Notes in Computer Science*, pages 6–13. Springer Berlin / Heidelberg, 2011.

[61] Dirk Holz, Stefan Holzer, Radu Bogdan Rusu, and Sven Behnke. Real-time plane segmentation using rgb-d cameras. In T. Röfer, N. M. Mayer, J. Savage, and U. Saranlı, editors, *RoboCup 2011: Robot Soccer World Cup XV*, volume 7416 of *LNCS*, pages 306–317. Springer Berlin Heidelberg, 2012.